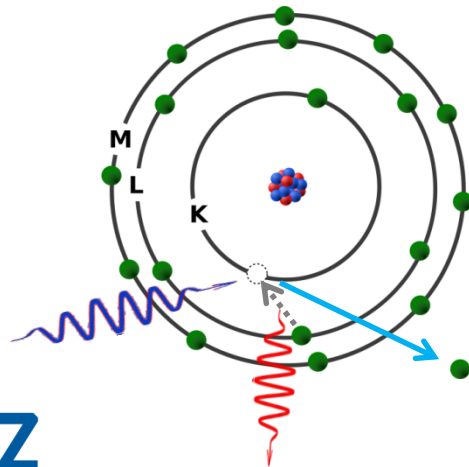
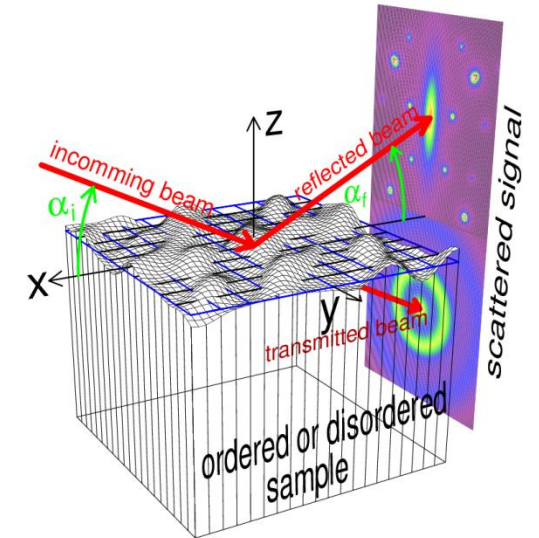
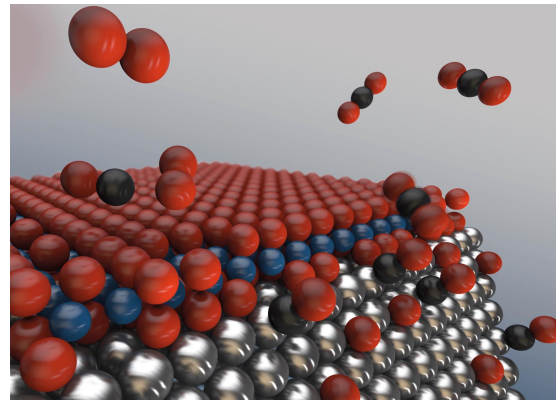
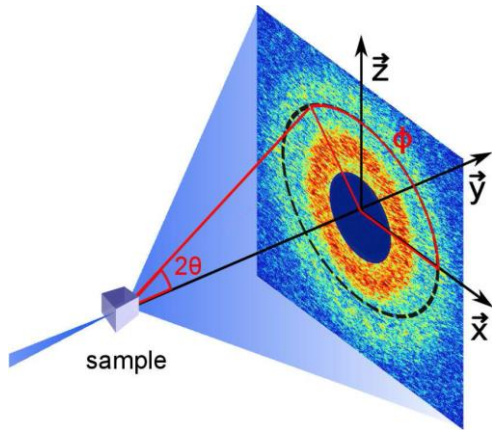


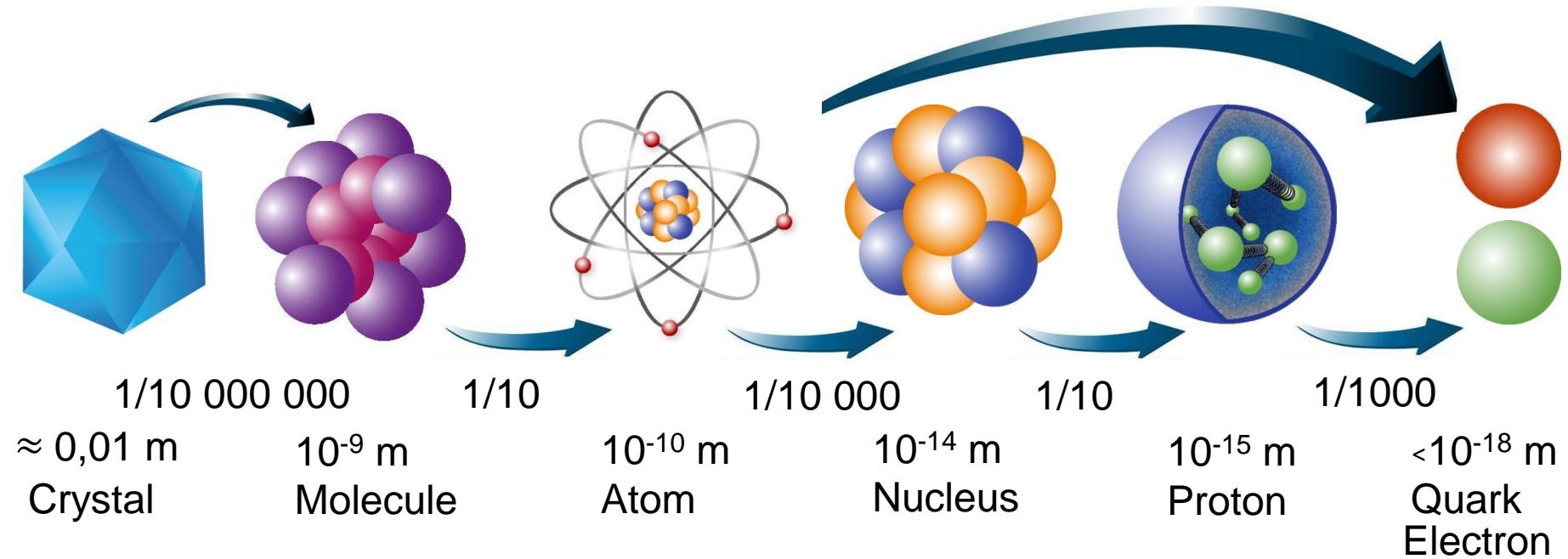
Exploring properties of the microcosm with brilliant X-rays



Wolfgang Drube

**Deutsches Elektronen-Synchrotron DESY
Hamburg, Germany**

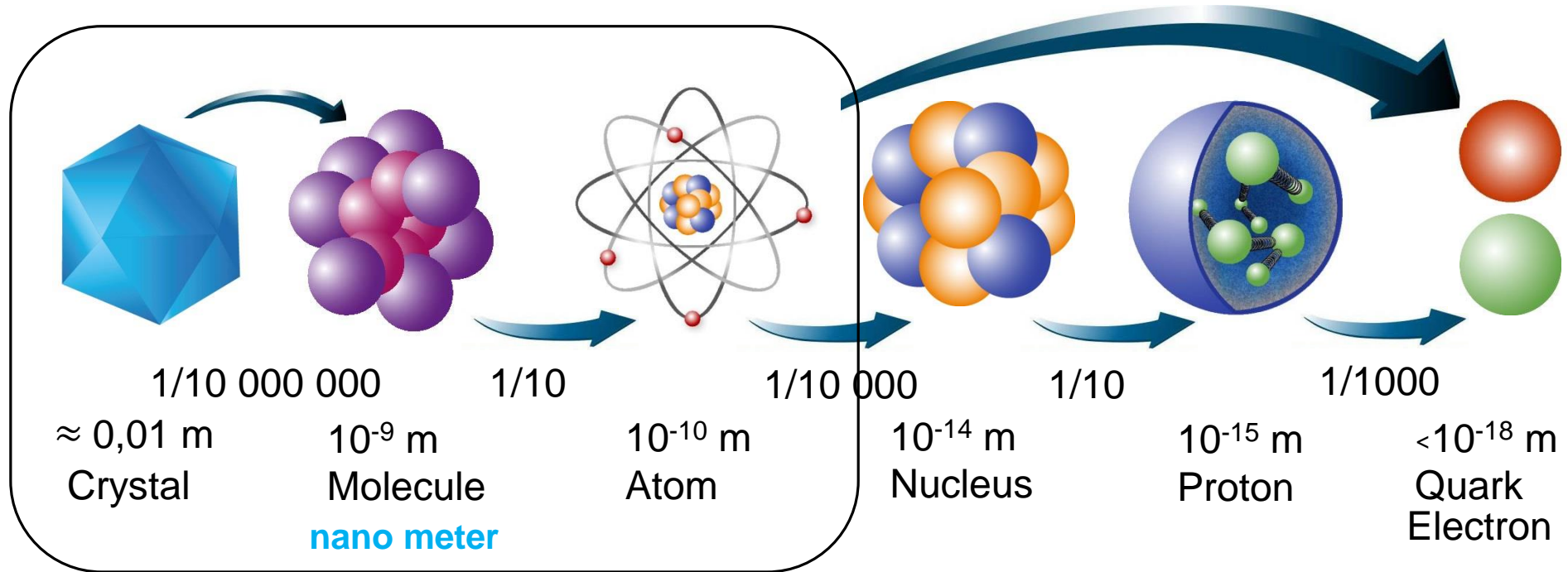
Building blocks of matter



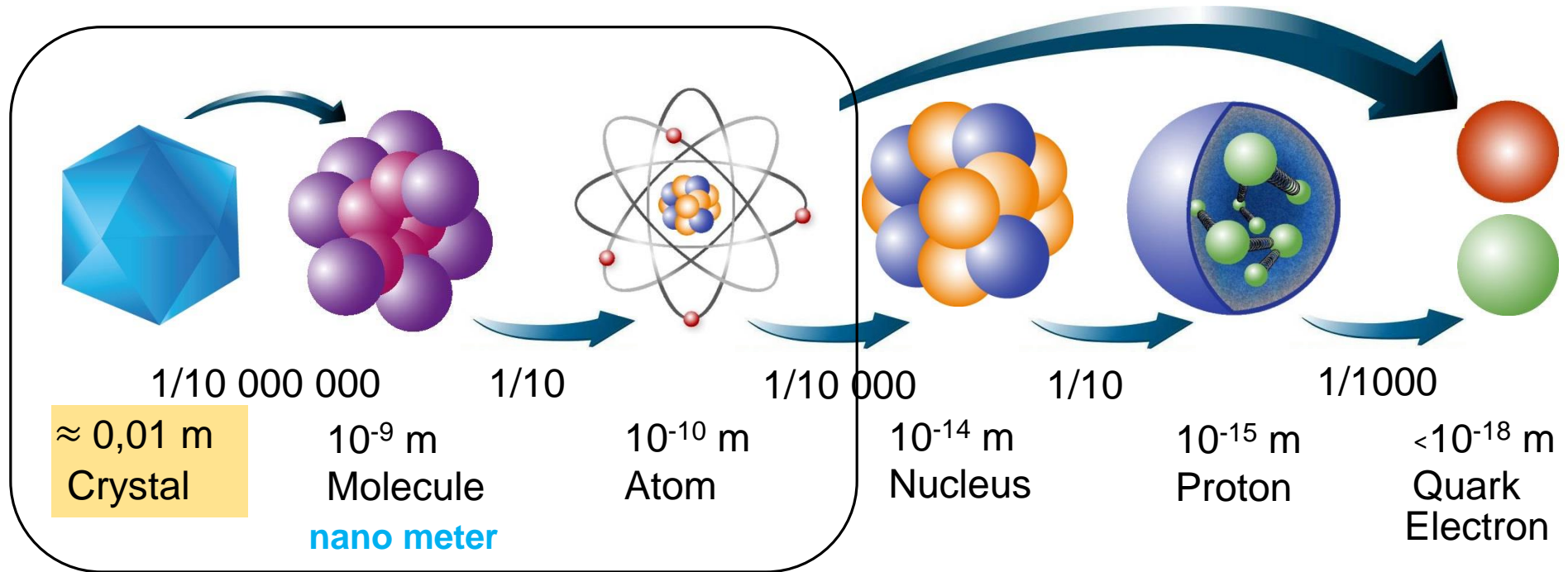
Pin head $10^{-3} \text{ m} = 0,001 \text{ m}$

Electron $10^{-18} \text{ m} = 0,000\,000\,000\,000\,000\,000\,001 \text{ m}$

Building blocks of matter



Building blocks of matter



Salt: NaCl



Sugar (sucrose): $\text{C}_{12}\text{H}_{22}\text{O}_{11}$

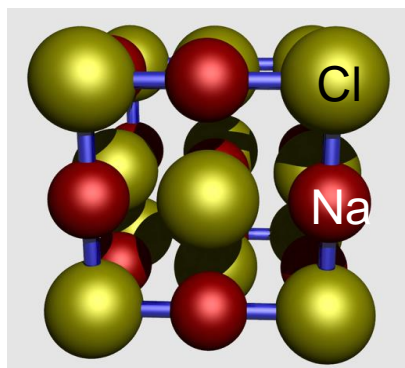
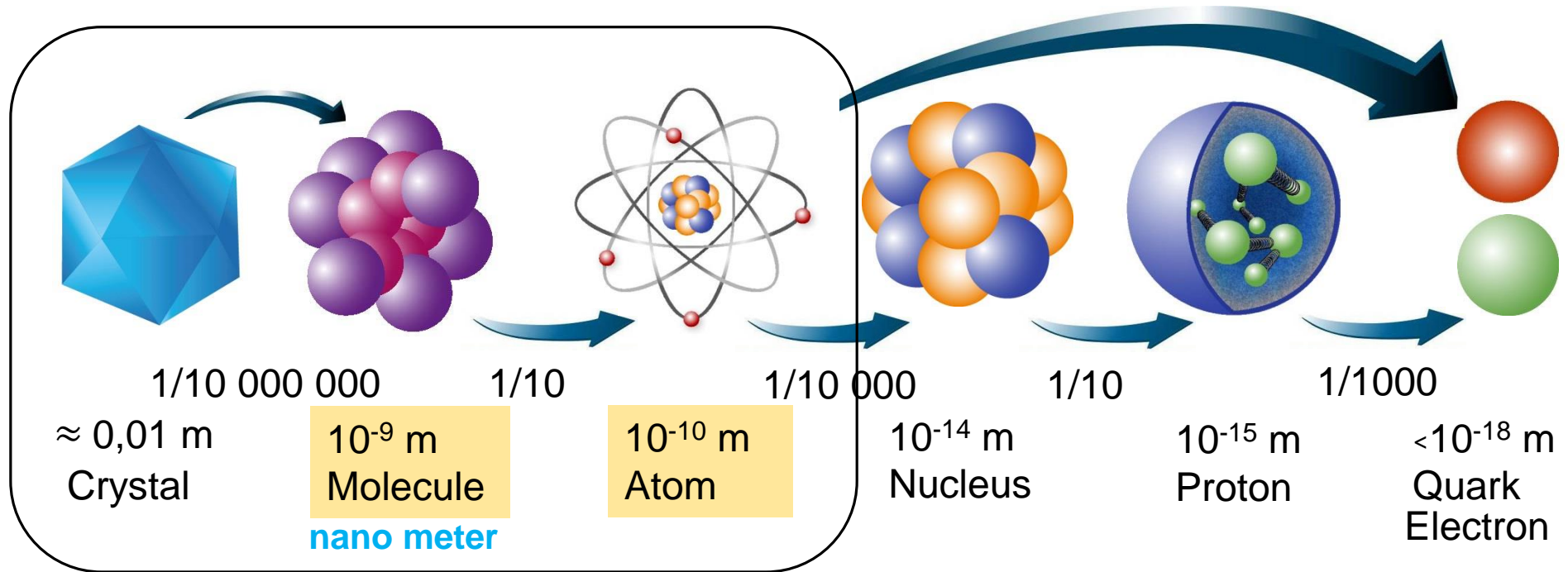


Diamond: C

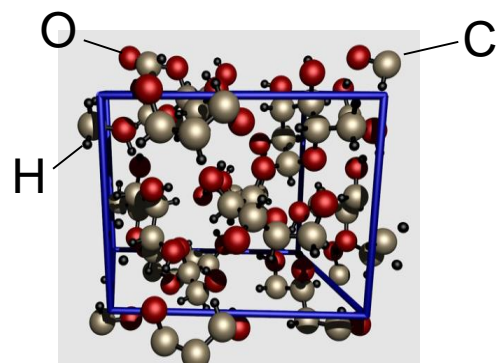


Rock crystal (quartz): SiO_2

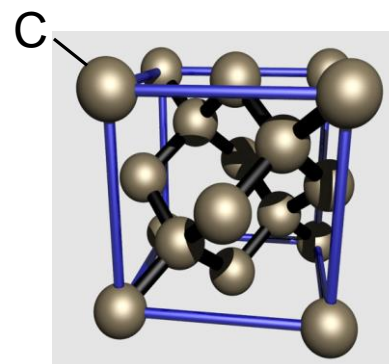
Building blocks of matter



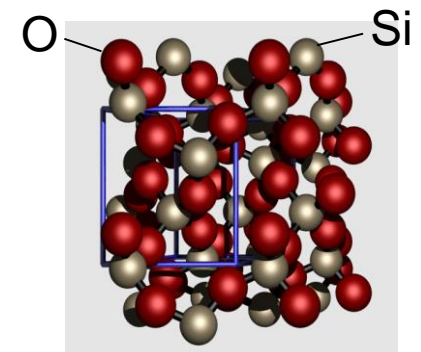
Salt: NaCl



Sugar (sucrose): $C_{12}H_{22}O_{11}$



Diamond: C

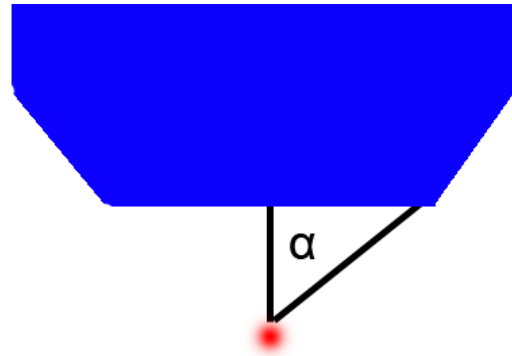


Rock crystal (quartz): SiO_2

Light as a probe: „zoom in“ with a microscope

(source: wikipedia)

Resolution of an optical microscope



smallest separation d
of two lines to be
distinctly visible:

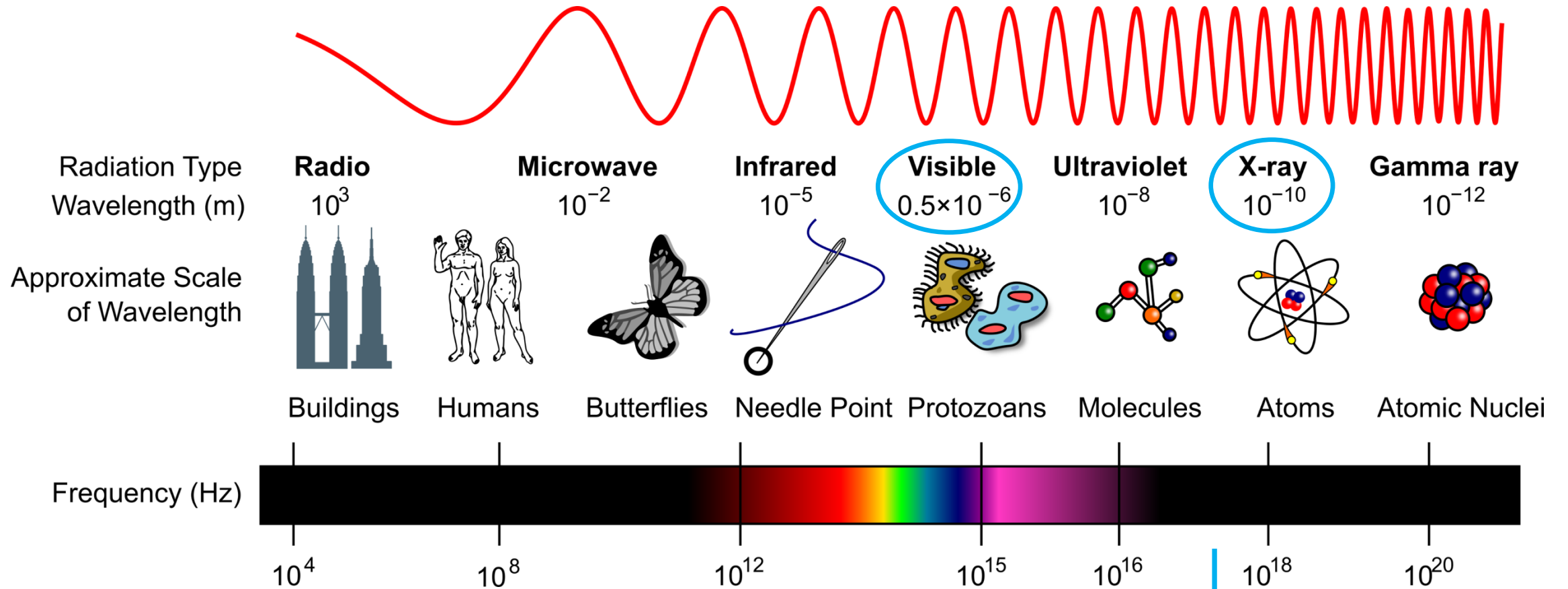
$$d = \frac{\lambda}{(2)n \sin \alpha}$$

Index of refraction: $n \sim 1$



Ernst Abbe
(Jena , \approx 1870)

Electromagnetic waves



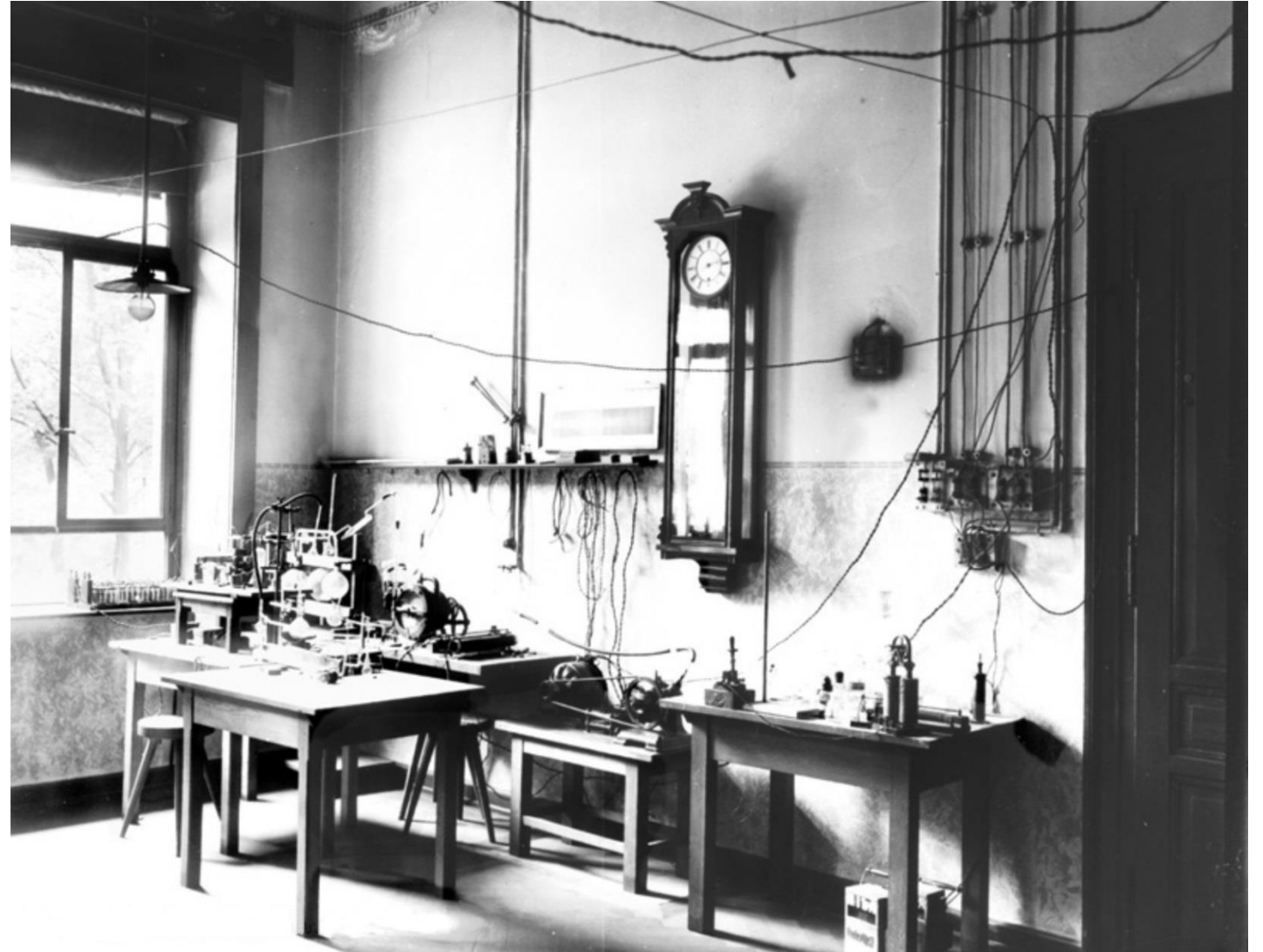
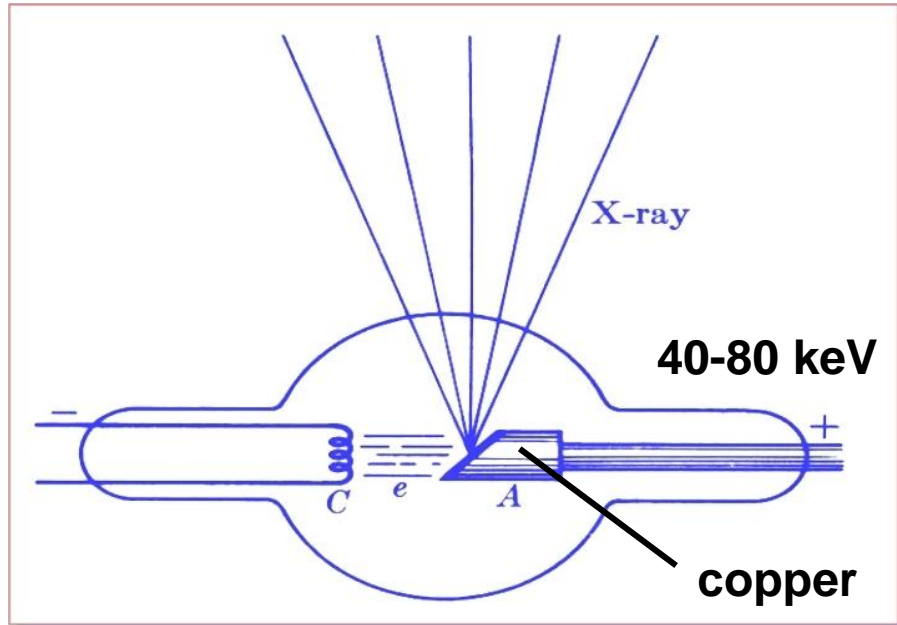
graphics adapted from:
<https://commons.wikimedia.org/wiki/User:Inductiveload>

10 keV (energy)
 10 000 electron volt

Discovery of X-rays



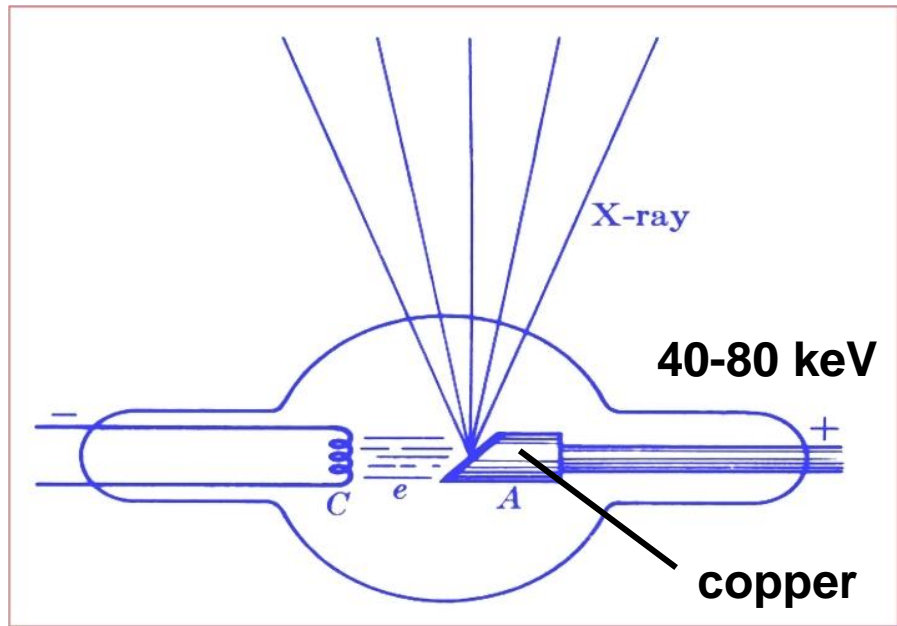
Discovered by
Wilhelm Conrad Röntgen
in Würzburg 1895
(First Nobel prize 1901)



Discovery of X-rays



Discovered by
Wilhelm Conrad Röntgen
in Würzburg 1895
(First Nobel prize 1901)



X-rays can penetrate (rather thick) material)



X-rayed hand of his wife
Anna Bertha Ludwig
(22. December 1895)

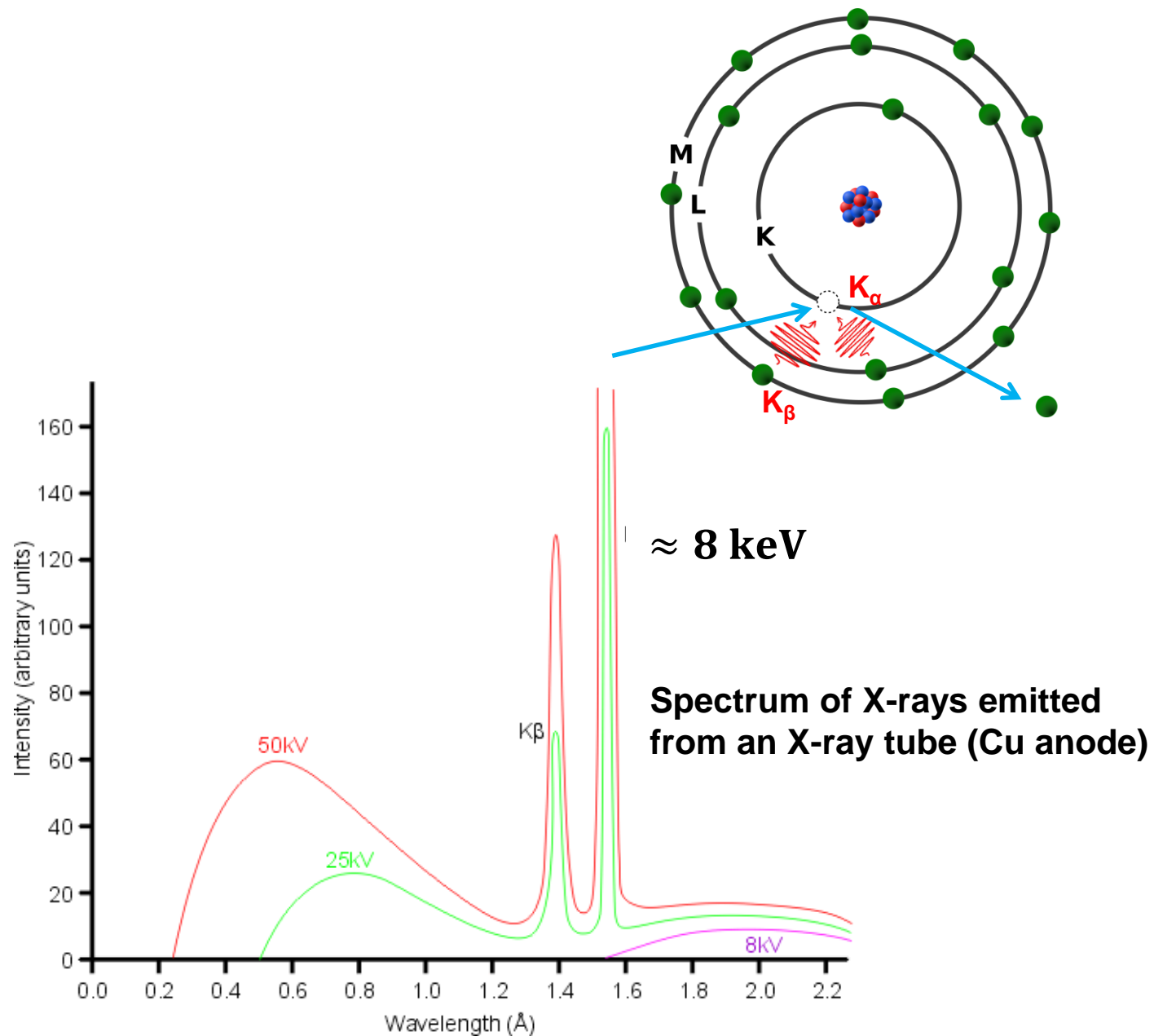
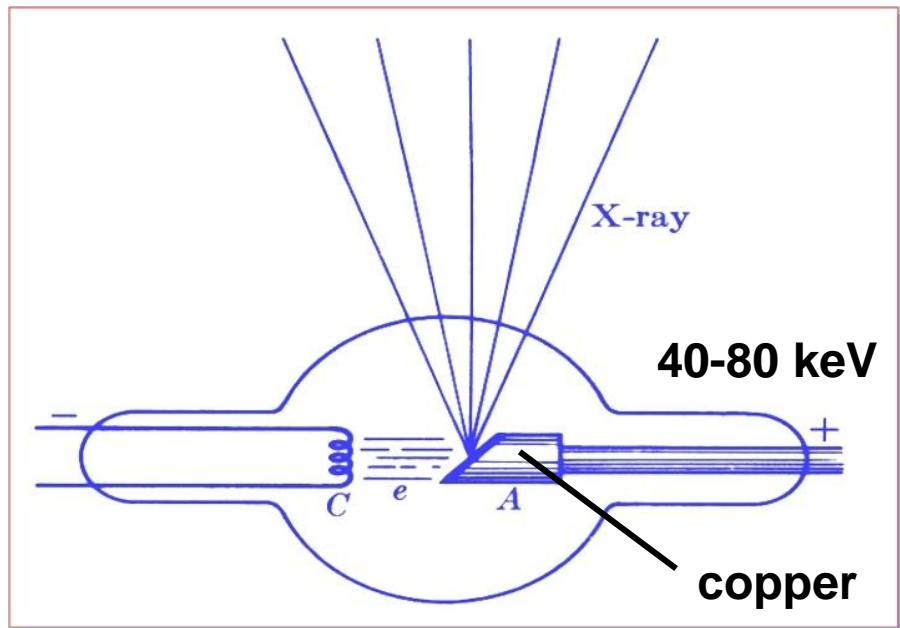


the image contrast is caused by
different X-ray absorption in
soft tissue and bones

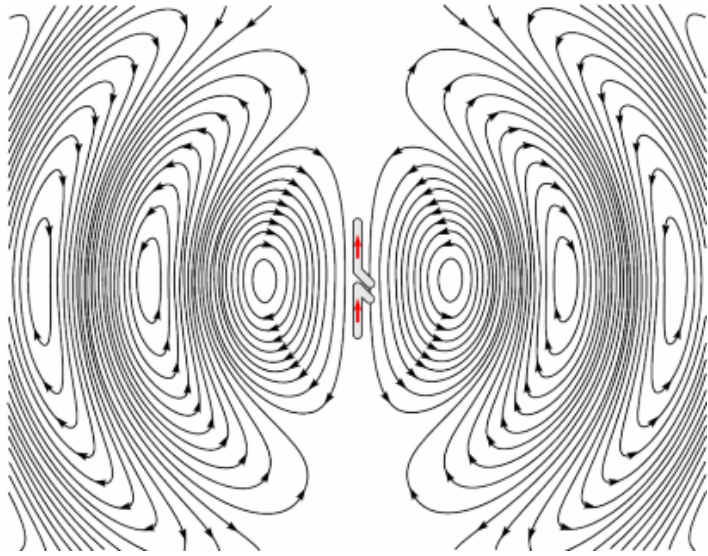
Discovery of X-rays



Discovered by
Wilhelm Conrad Röntgen
in Würzburg 1895
(First Nobel prize 1901)



Accelerated electrons emit radiation

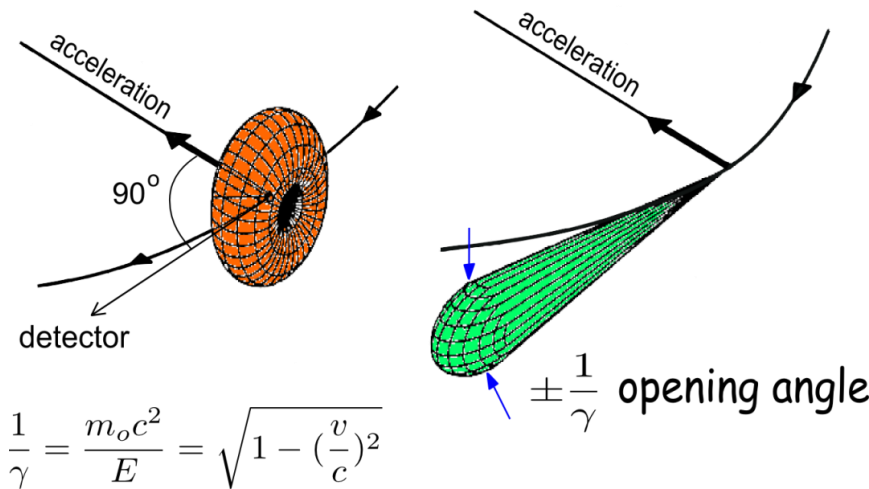


“very fast” electrons (~ speed of light)

Lorentz-Transformation

Moving frame
of electron

Lab frame



$$\frac{1}{\gamma} = \frac{m_0 c^2}{E} = \sqrt{1 - \left(\frac{v}{c}\right)^2}$$

an accelerated charge emits
electromagnetic radiation

the angular distribution:
Hertz dipole

highly collimated !

opening angle $1/\gamma = 0.5 \text{ MeV}/6 \text{ GeV} \approx 0.005^\circ$
(PETRA III storage ring) 80 μrad

In practice:

large particle accelerators:

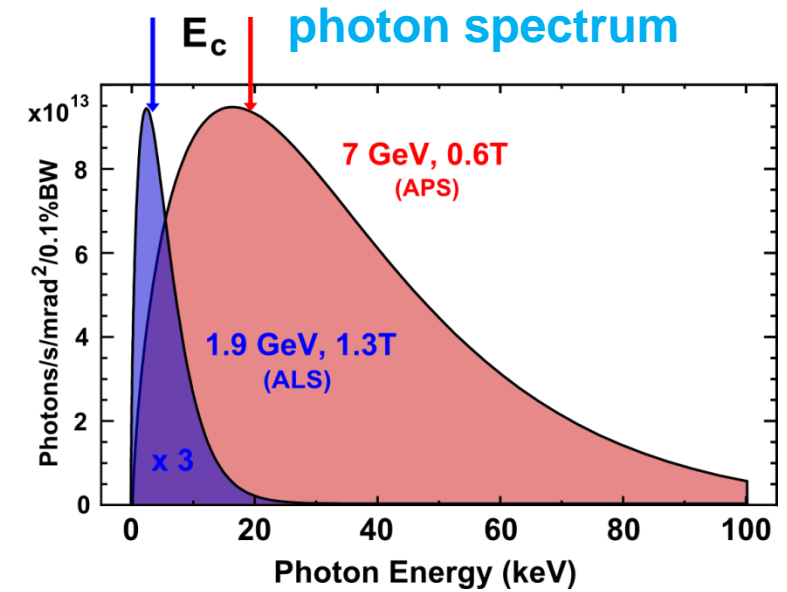
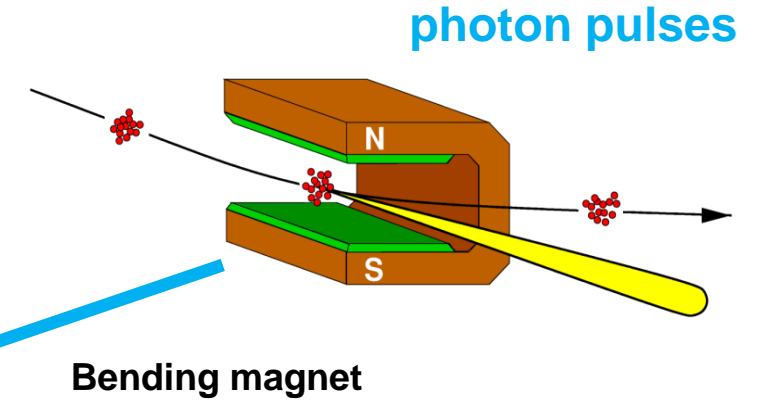
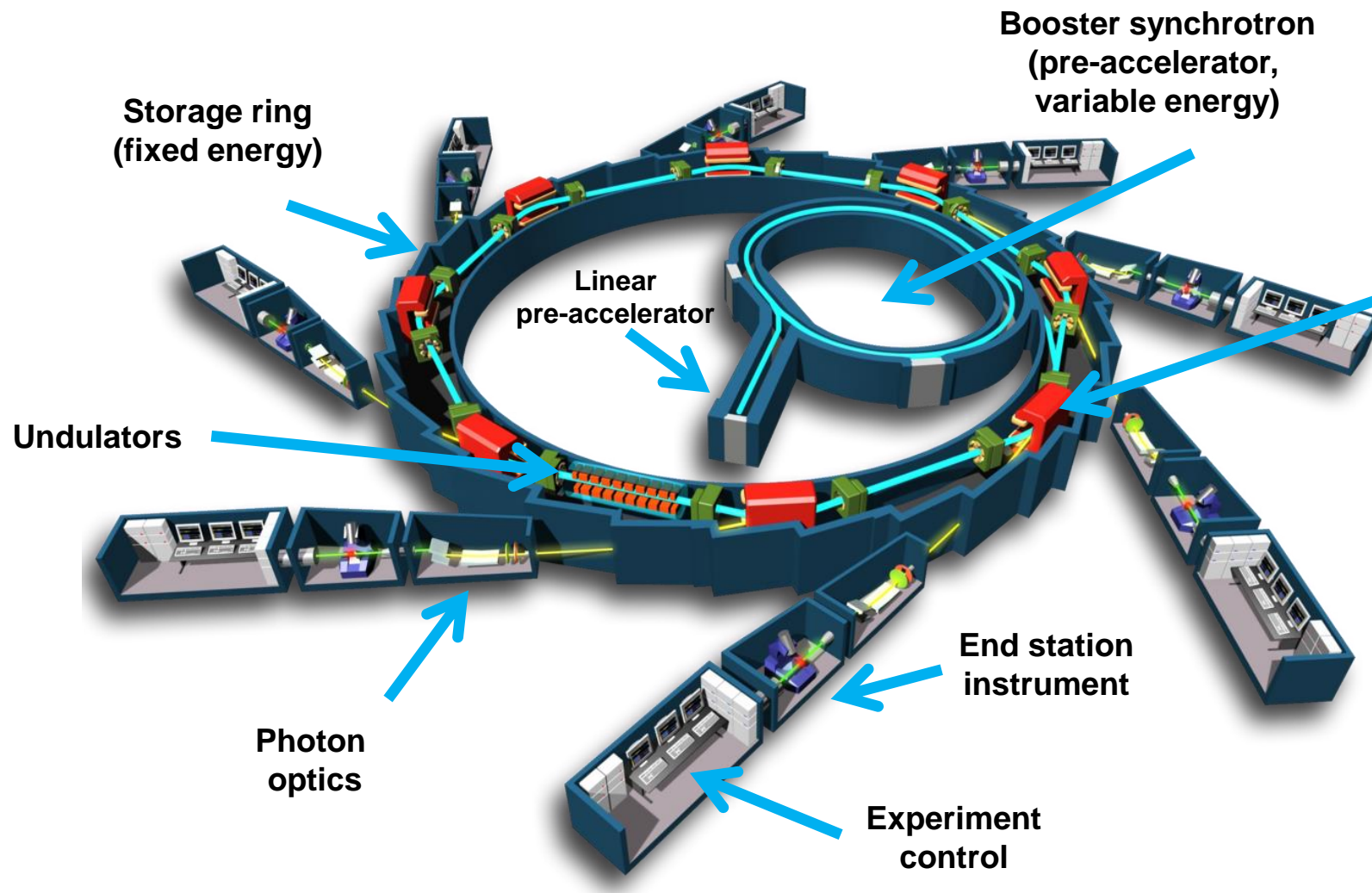
circular motion in an
electron storage ring

radiated power P_s (Lamor)

$$P_s = \frac{e^2 c}{6\pi\epsilon_0 (m_0 c^2)^4} \frac{E^4}{R^2}$$

electron energy loss per turn $\Delta E \sim E^4/R$
 $E \sim \text{GeV}$ $R \sim \text{m}$

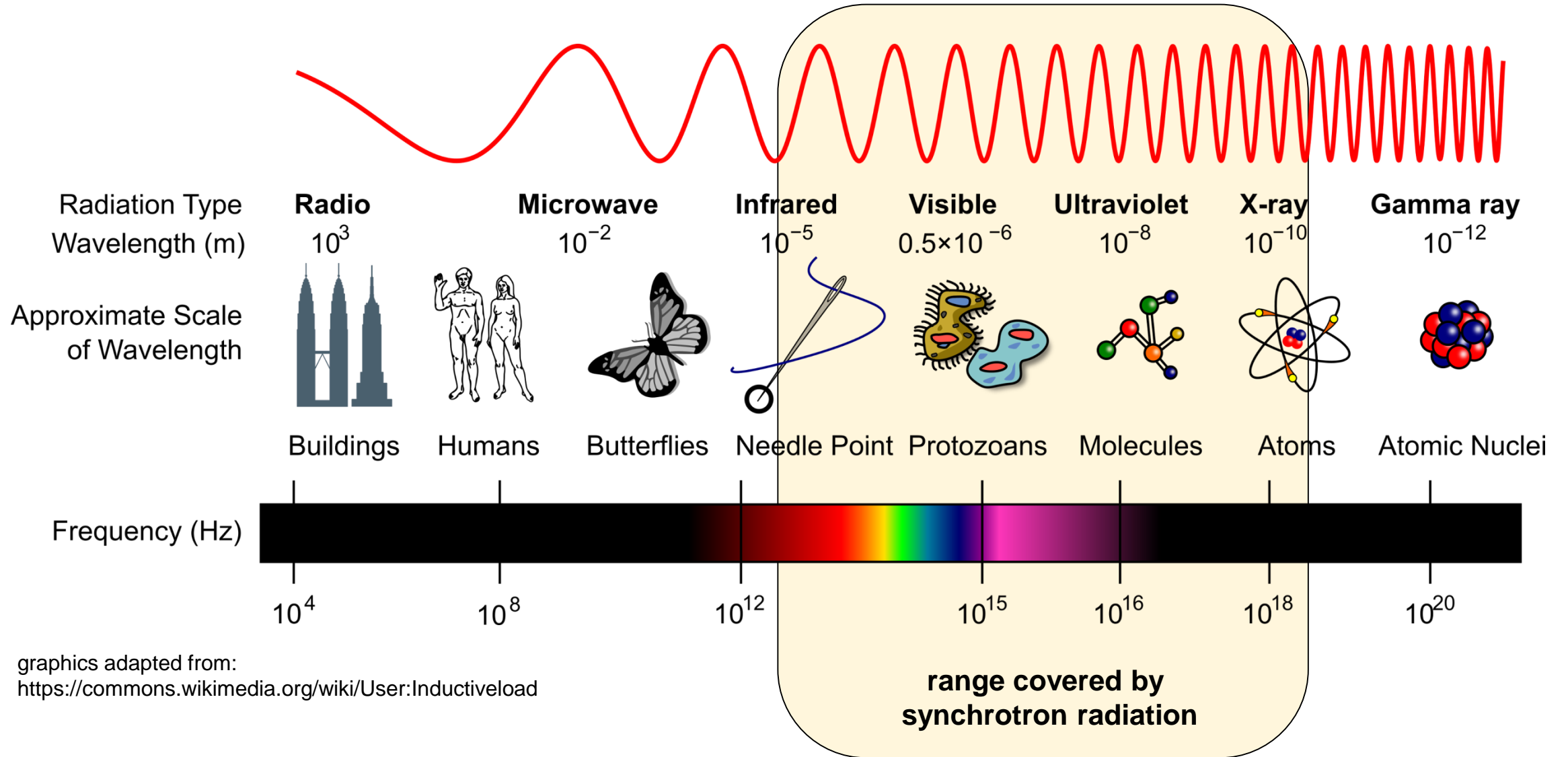
Schematic Synchrotron Radiation Facility



$$E_c \text{ (keV)} = 0.665 \cdot E_e^2 \text{ (GeV)} \cdot B_0 \text{ (T)}$$

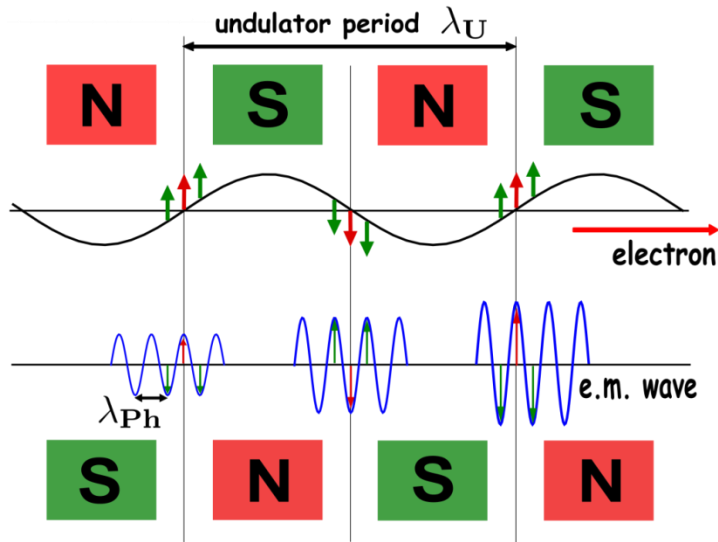
Big machines: circumference 300 – 2300 m

Electromagnetic waves



graphics adapted from:
<https://commons.wikimedia.org/wiki/User:Inductiveload>

Intense X-ray beams from „undulators“



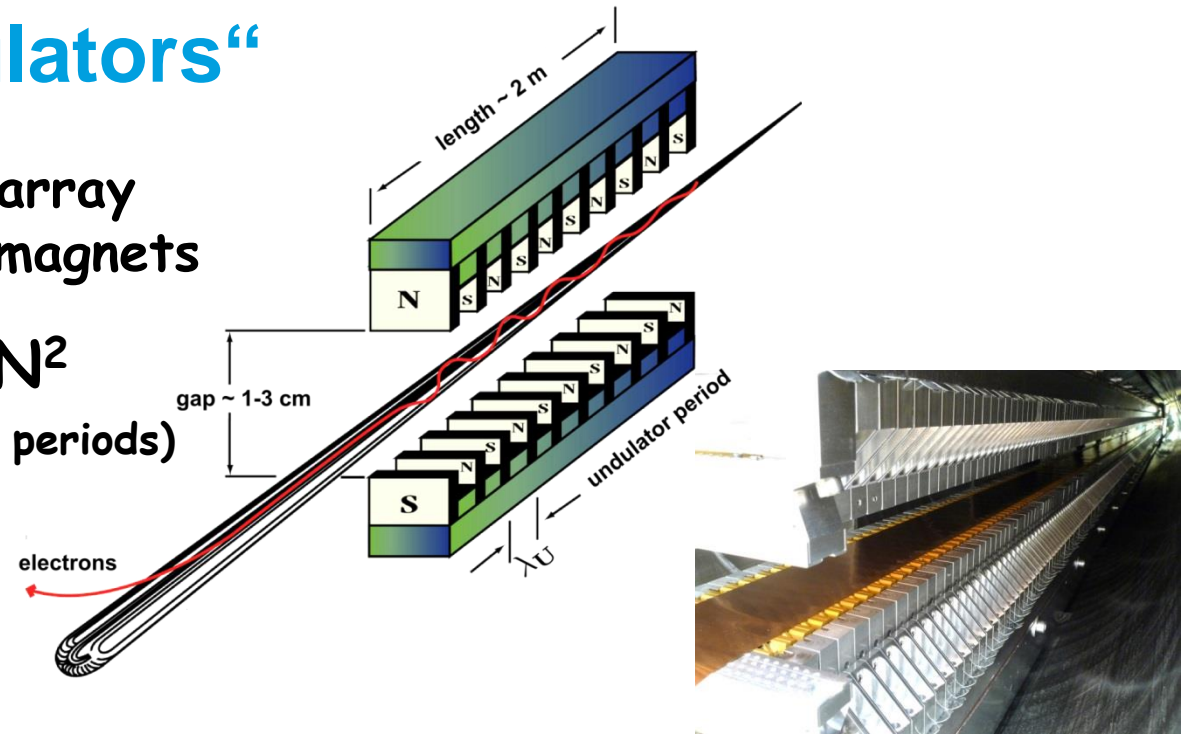
$$\lambda_{ph} = \frac{\lambda_u}{2\gamma^2} \left(1 + \frac{K^2}{2} \right)$$

$$K = 0.934 \lambda_u [\text{cm}] B[\text{T}]$$

periodic array
of strong magnets

$$I \sim N^2$$

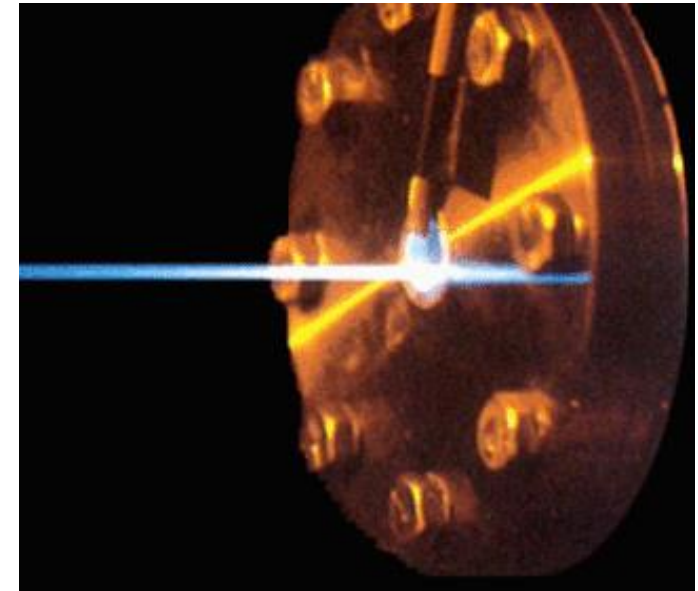
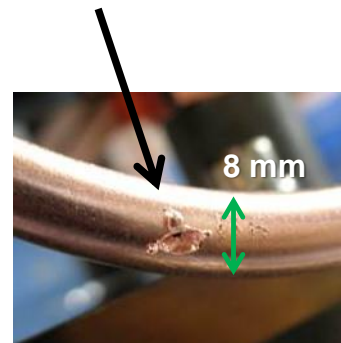
(N = no. of periods)



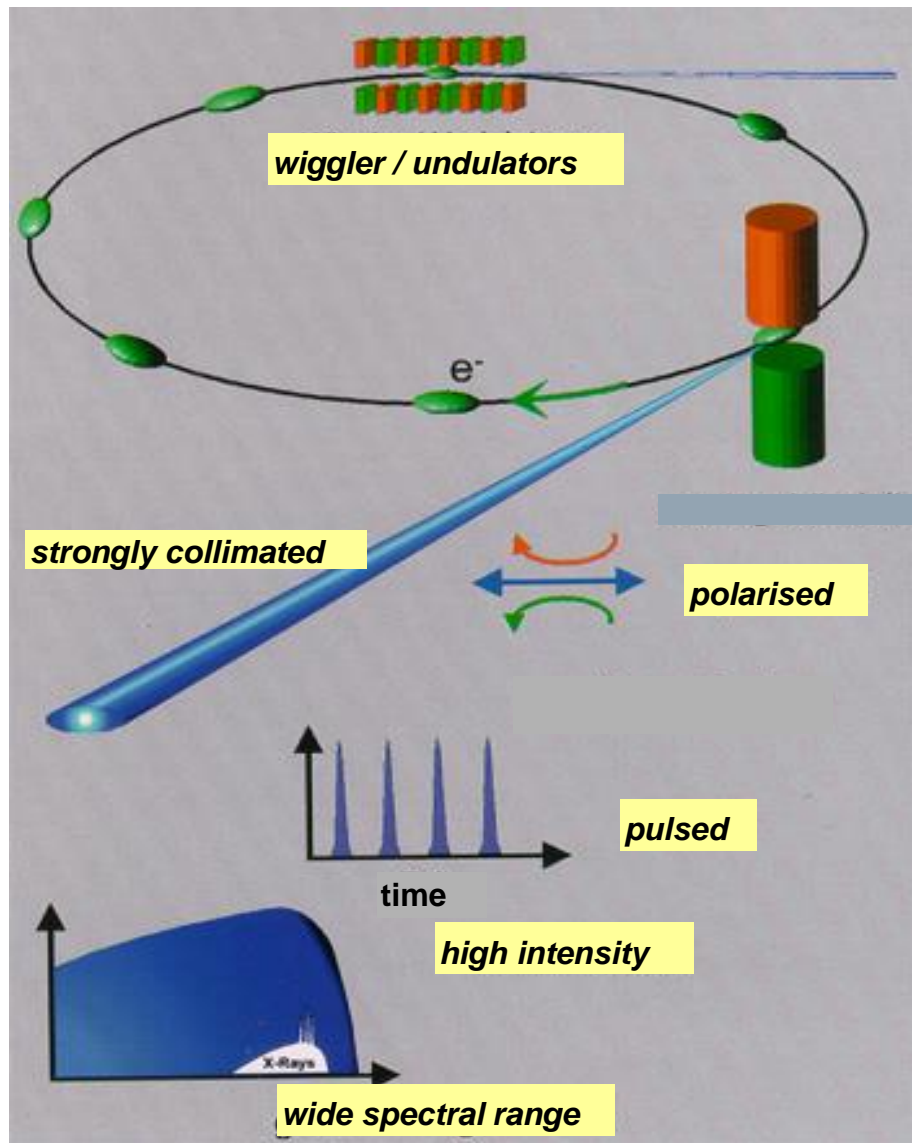
Light power:

Sunlight on earth: $P_{sol} \approx 0.0013 \text{ W/mm}^2$

SR undulator: $P_{SR} \approx 8000 \text{ W/mm}^2$

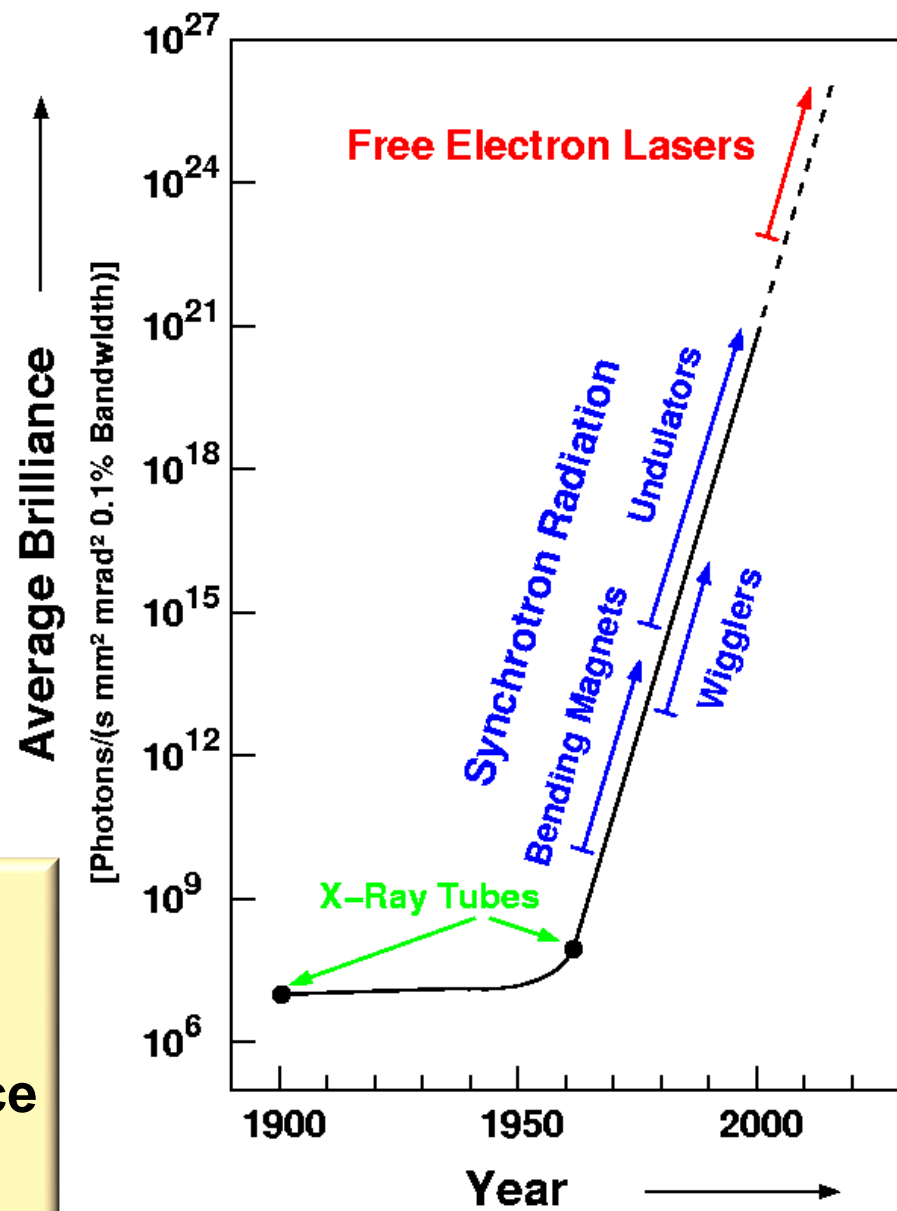


Synchrotron radiation at a glance



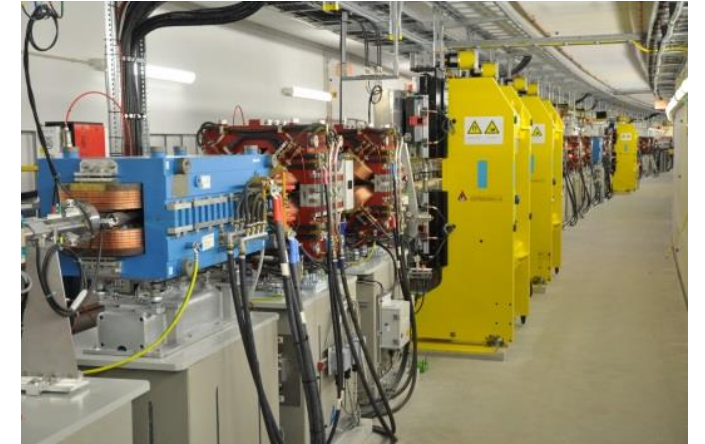
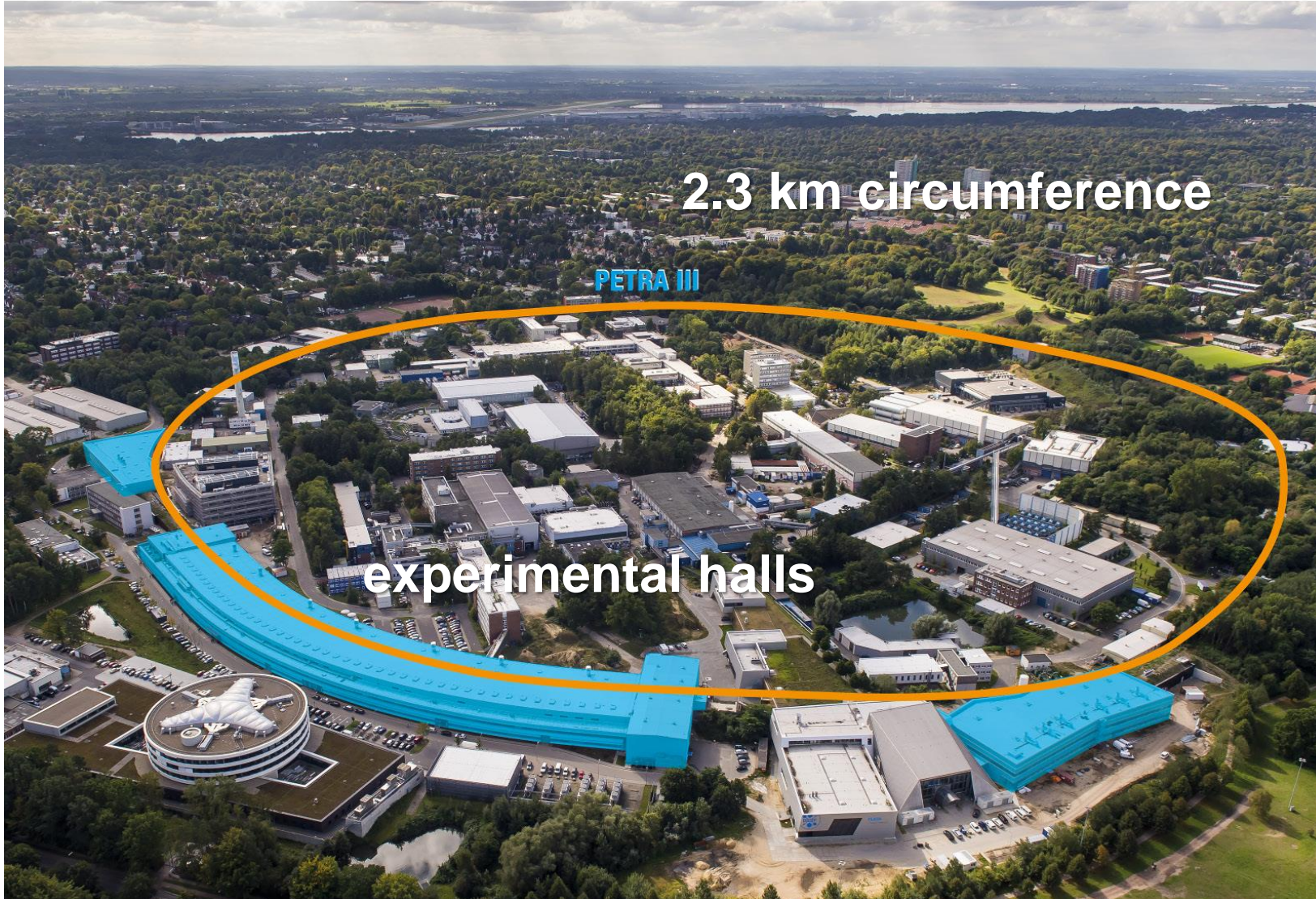
high intensity
>10 000 times
 more intense
 than
 the most modern
 X-ray lab source

strong collimation
 beam size (vertical)
 from undulator source
~1 mm at 100 m !
 (without focusing)



10.000 x "more light"
 per decade since 1965

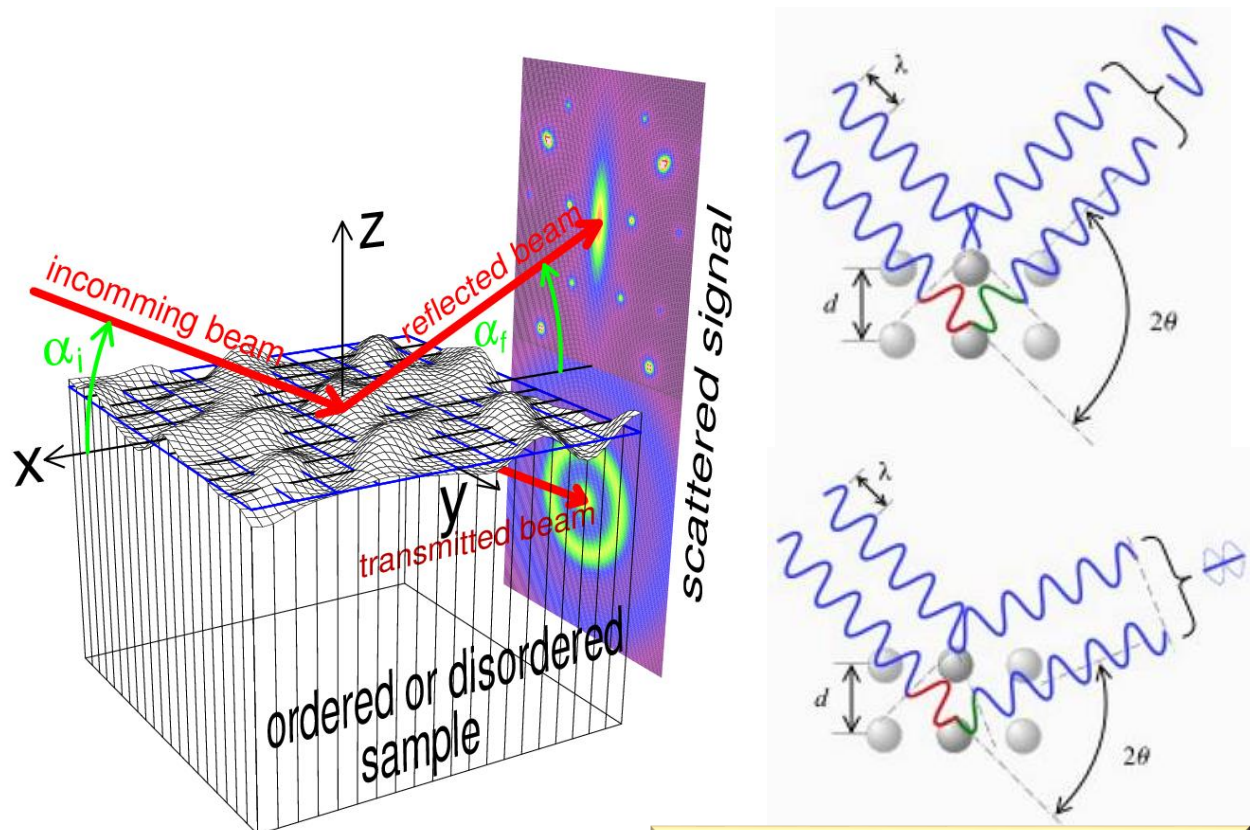
Synchrotron radiation facility (PETRA III in Hamburg)



X-rays: excellent probe for the study of material properties

(Elastic) scattering, diffraction, imaging:

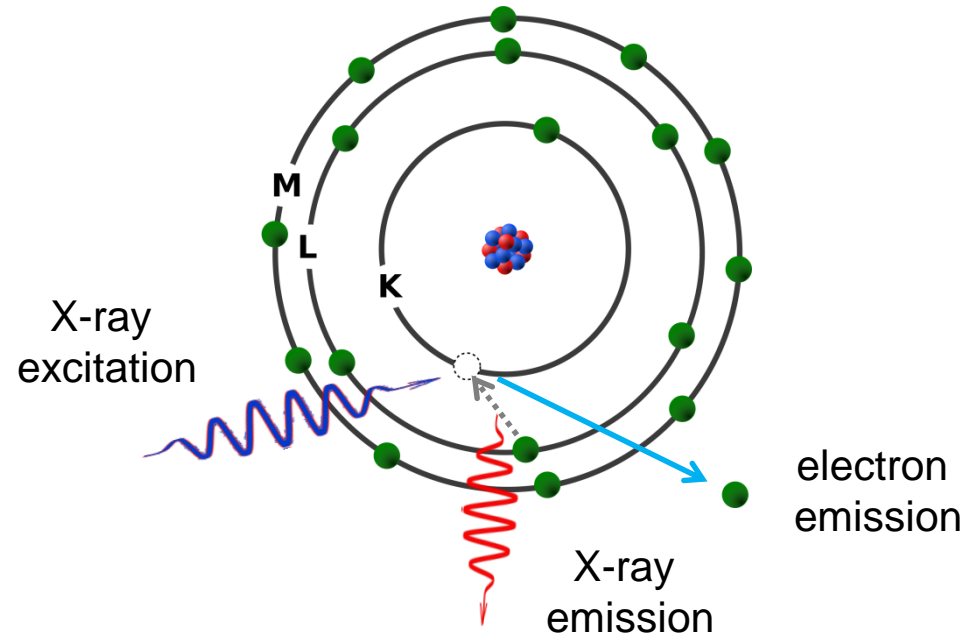
geometrical atomic structure, nano particle shapes



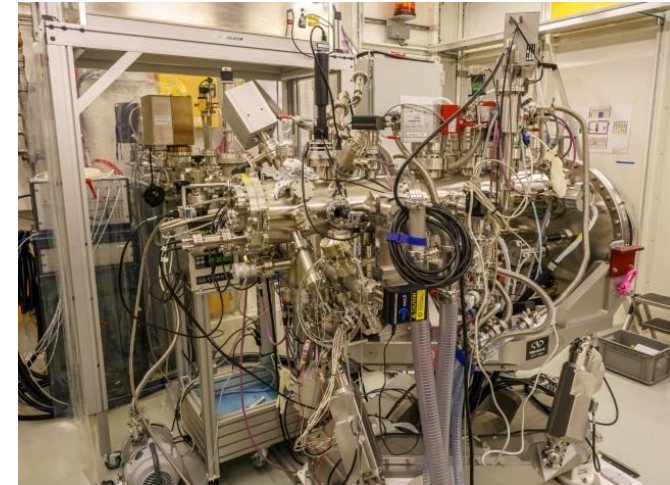
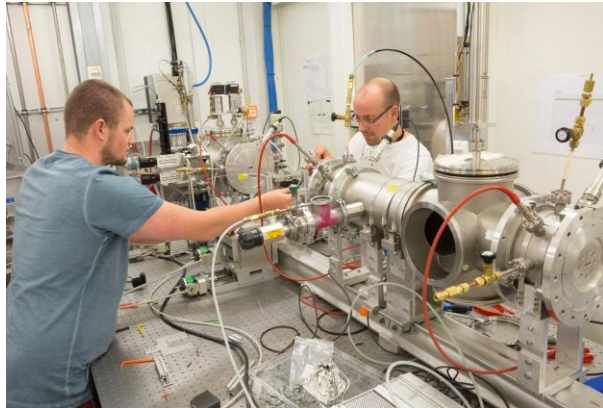
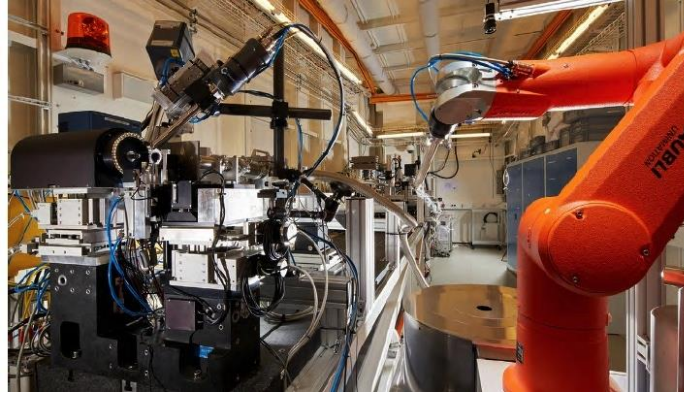
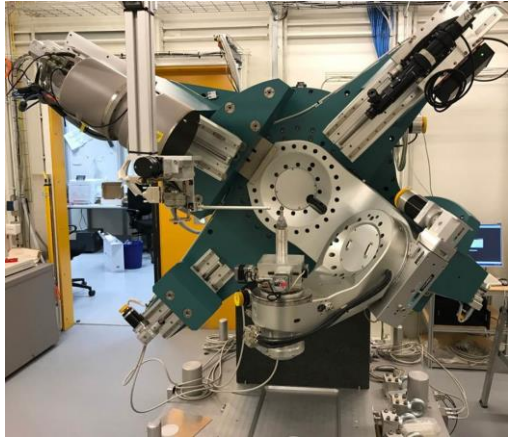
wave interference from atomic scatterers
→ structural information

(Inelastic) atomic excitations:

elemental composition and distribution, chemical bonding, electronic structure (magnetism, super-conductivity, ...)



Specialized experimental stations for different applications



X-rays uncover hidden master pieces

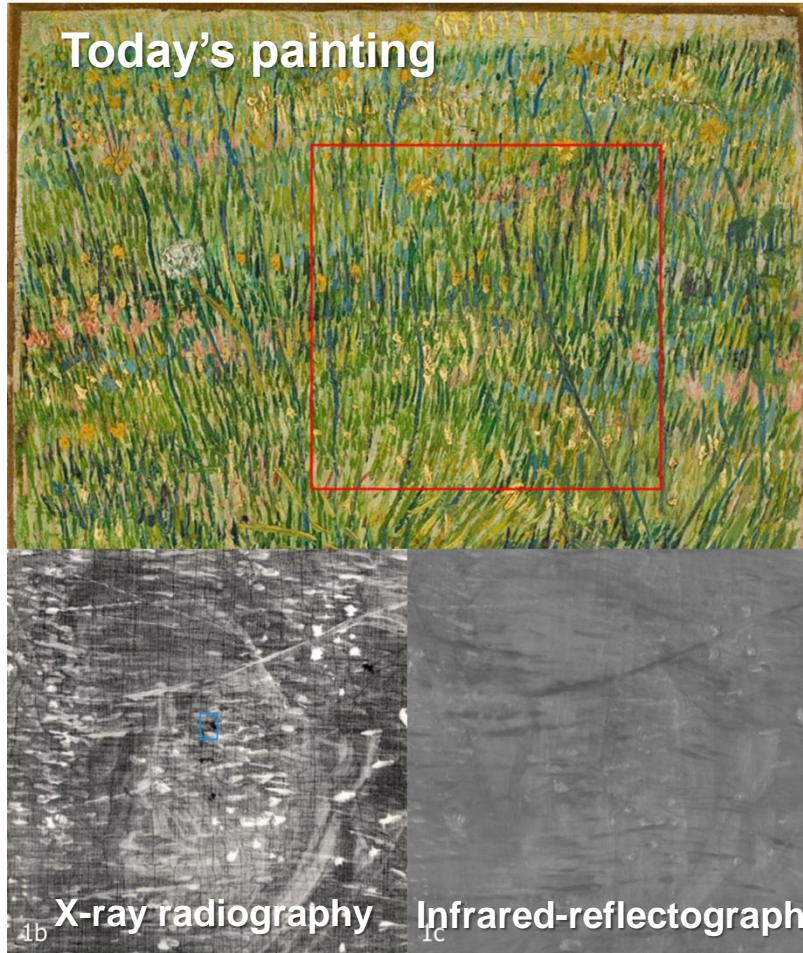
Vincent van Gogh

Patch of Grass

Paris, 1886

Kroeller Mueller Museum

Otterlo, the Netherlands



Let's begin with an example relating to cultural heritage

van Gogh often re-used his canvases (by overpainting)

X-rays uncover hidden master pieces

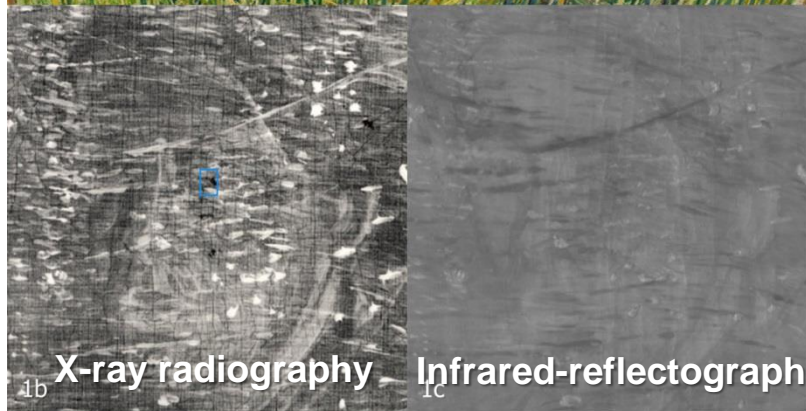
Vincent van Gogh

Patch of Grass

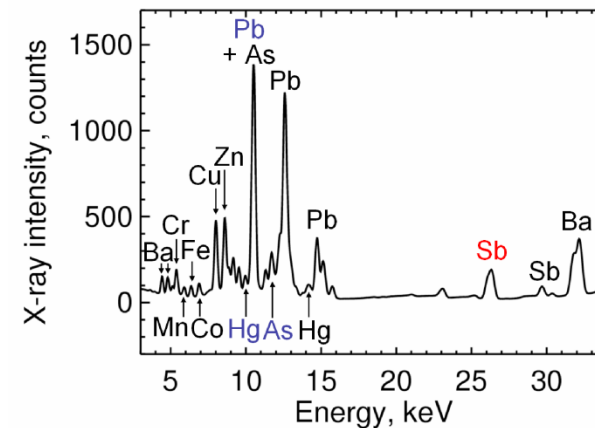
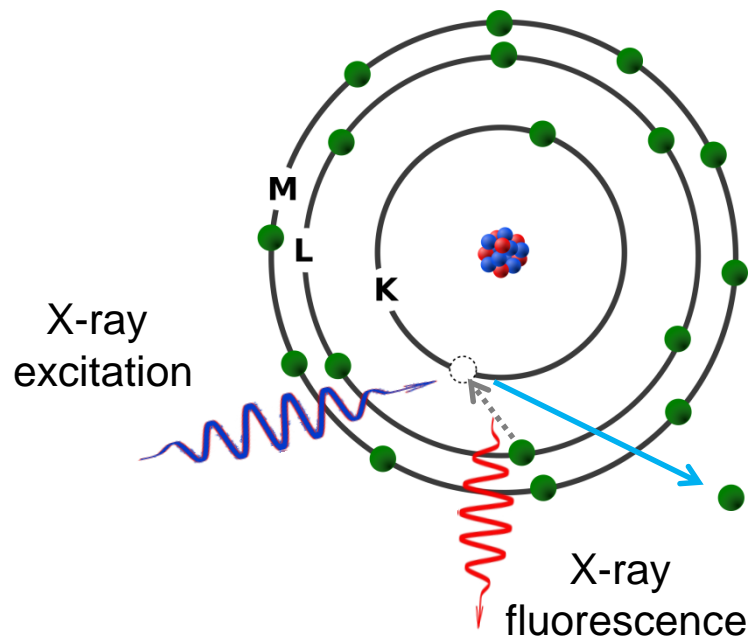
Paris, 1886

Kroeller Mueller Museum

Otterlo, the Netherlands



Idea:
study paint chemistry
by element selective
X-ray fluorescence



X-rays uncover hidden master pieces

Vincent van Gogh

Patch of Grass

Paris, 1886

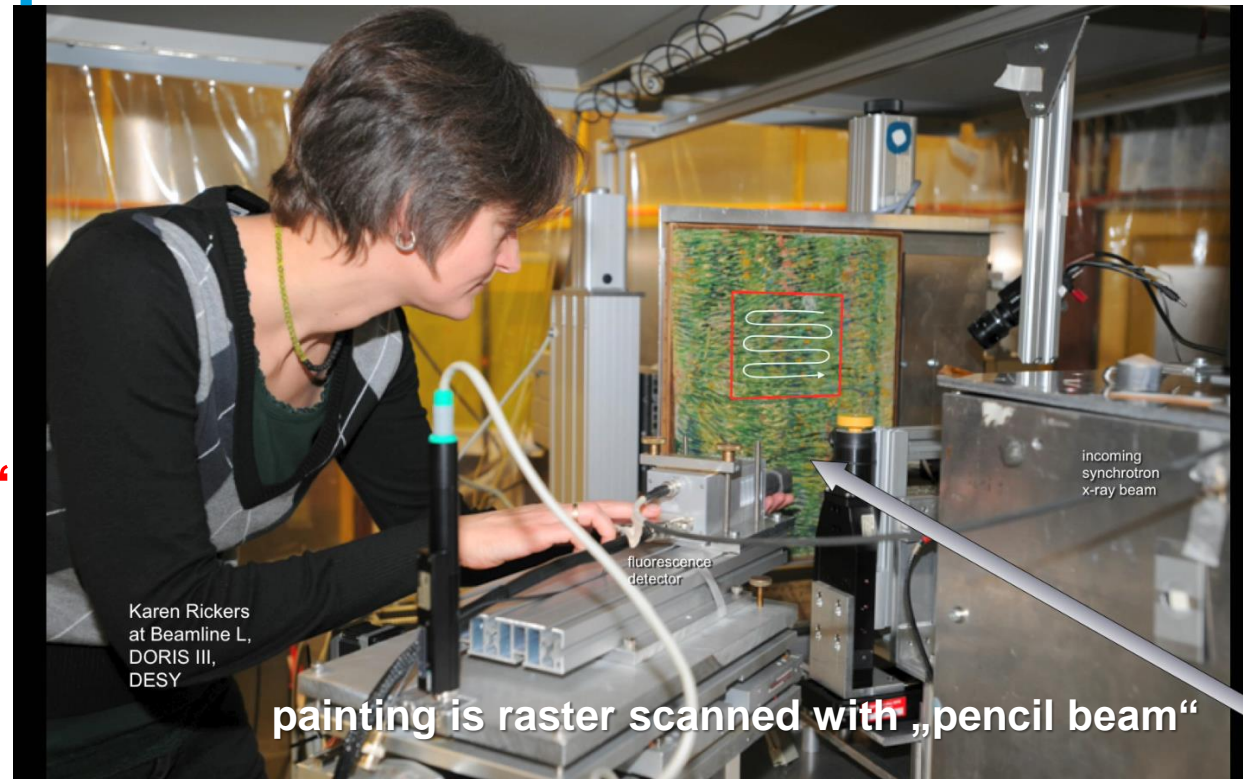
Kroeller Mueller Museum

Otterlo, the Netherlands

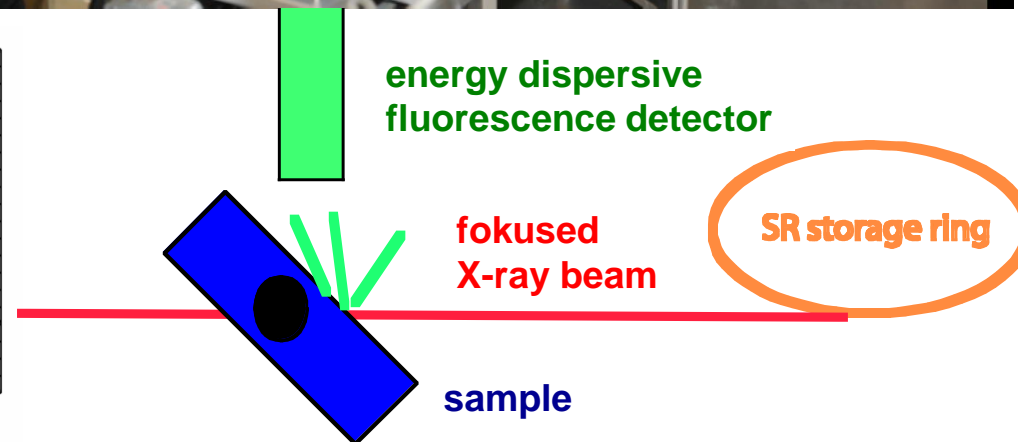
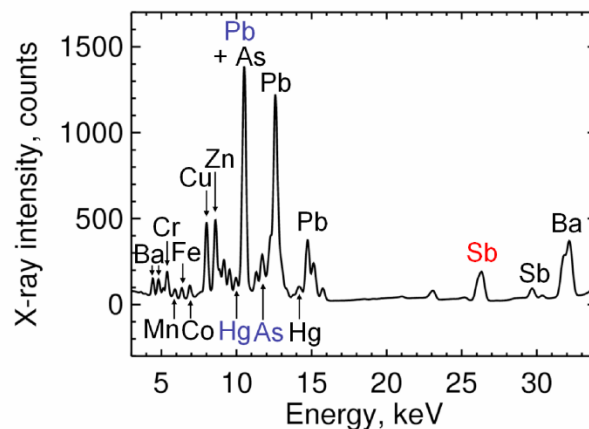
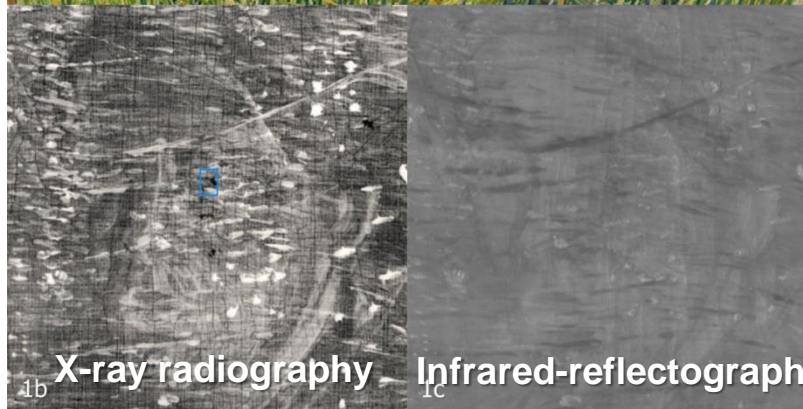


Today's painting

„pencil beam“
0.5x0.5mm²



Karen Rickers
at Beamline L,
DORIS III,
DESY

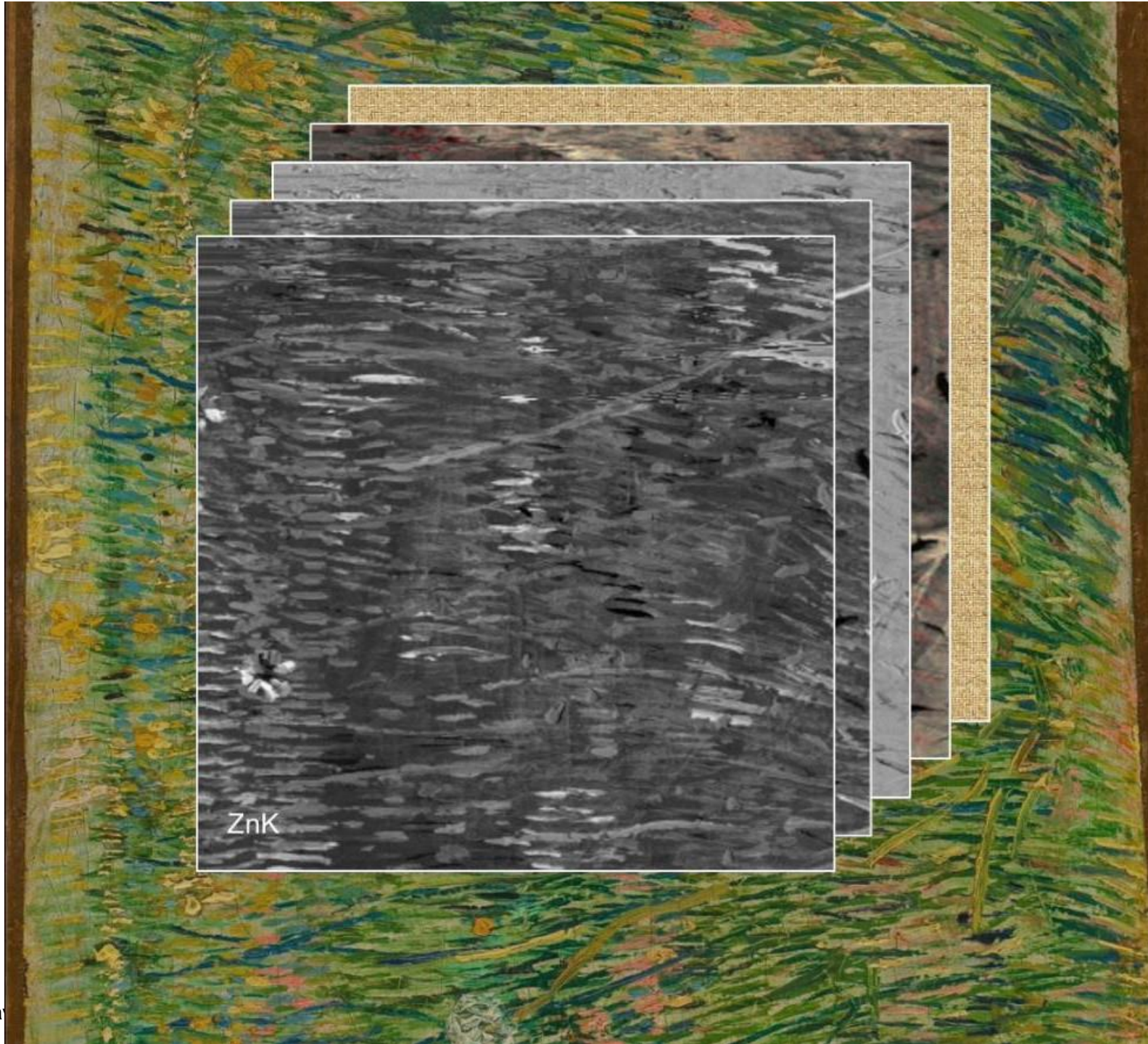


**view
marked
area
by paint
elements**



**view
marked
area
by paint
elements**

Zink



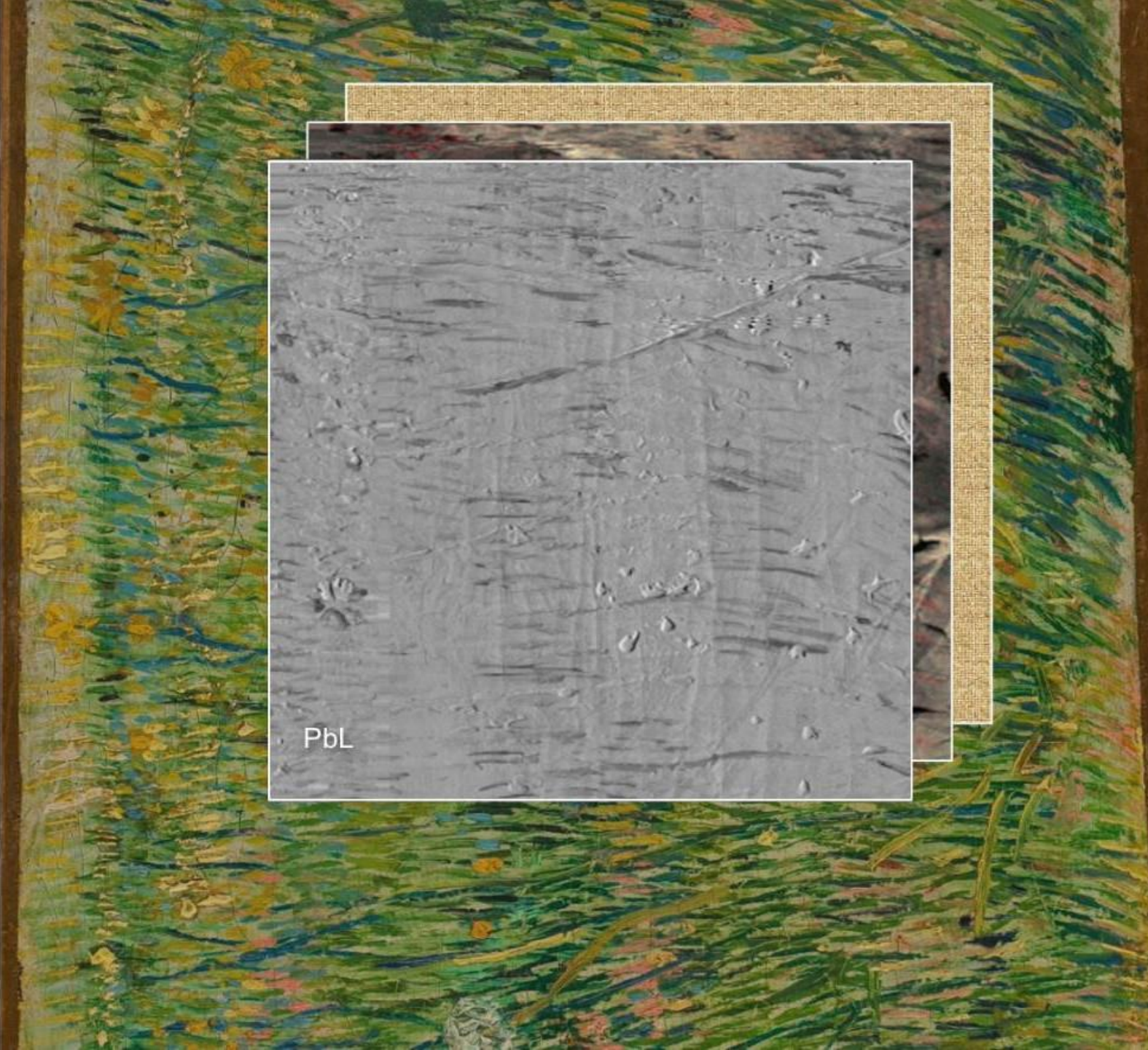
**view
marked
area
by paint
elements**

Barium



**view
marked
area
by paint
elements**

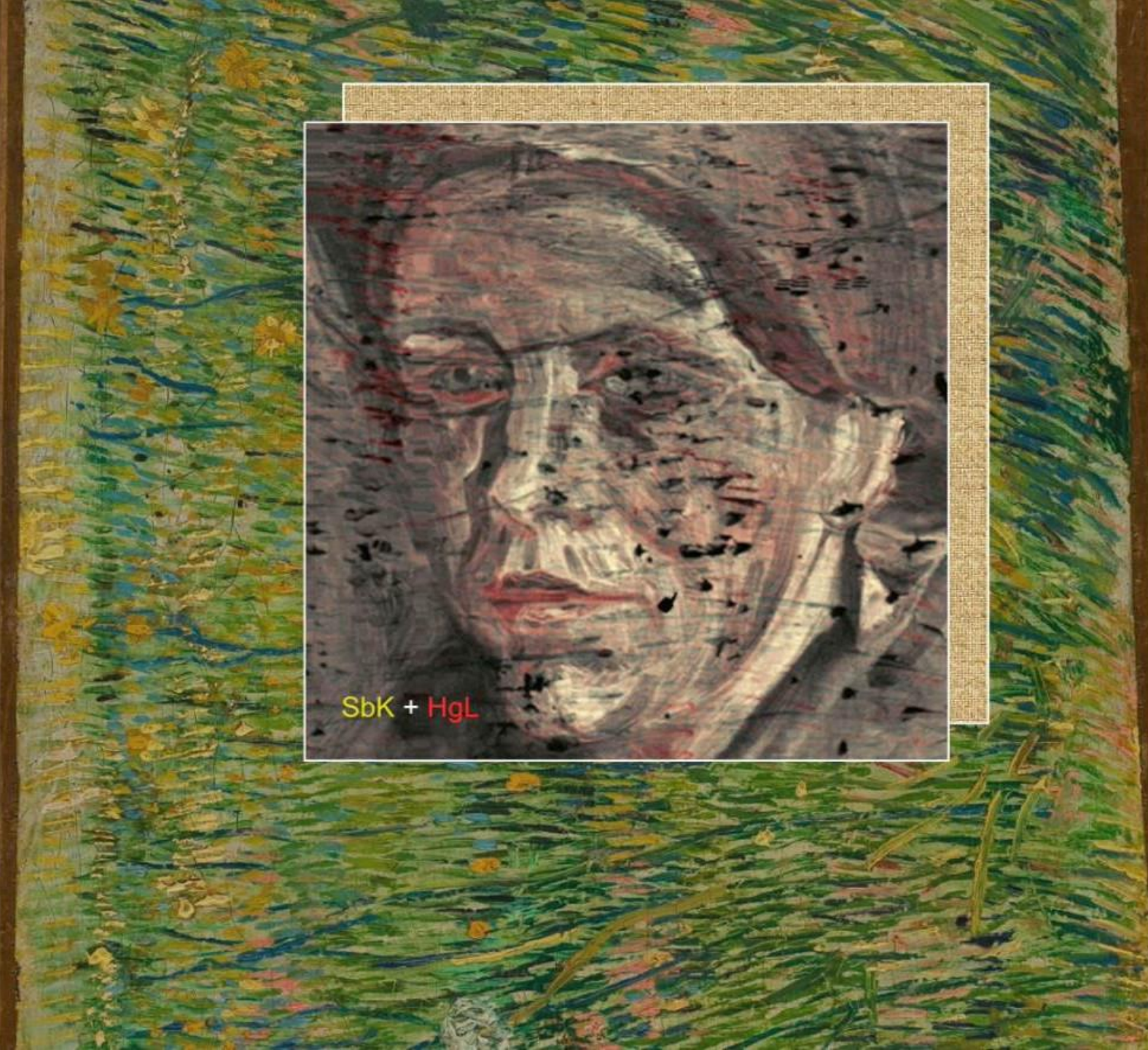
Lead



**view
marked
area
by paint
elements**

**Antimony
&
Mercury**

„Naples yellow“



X-rays uncover hidden master pieces

Nature News



GOT A NEWS TIP?
Send any article ideas for Nature's News section to newstips@nature.com

K. CAMPBELL/GETTY IMAGES

SNAPSHOT The hidden van Gogh

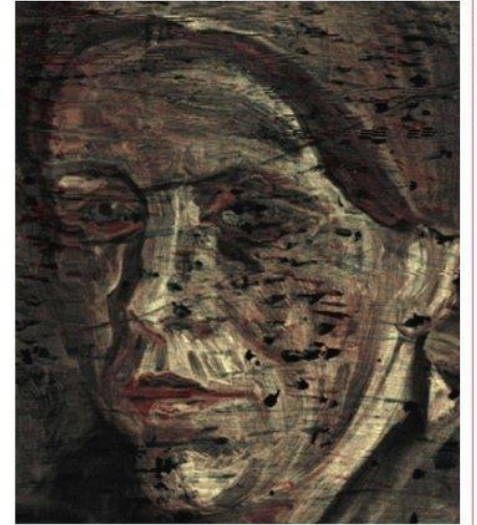
An unknown Vincent van Gogh painting of a woman's head has been revealed with X-ray technology. The painting is thought to have been made in 1884-85, during a period in which he painted several portraits of peasants in the Dutch village of Nuenen. The image was hidden beneath *Patch of Grass*, an unrelated landscape that van Gogh painted a year or two later when living in Paris.

Earlier X-ray studies revealed a faint, blurry shadow of a

doi:10.1021/ac800965g; 2008). The synchrotron's X-ray beam excites secondary X-rays from elements in the sample at characteristic wavelengths. The researchers mapped the distributions of cobalt, arsenic, lead and other metals in the hidden paint layers — all well-known components of pigments that were available at the time. Although the study did not identify all the pigments in the picture, it enabled the researchers to create the partial colour reconstruction shown here.

Van Gogh often re-used old canvases, partly in an effort to save money. Dik's team speculates that he took the

him to Paris, old have seemed unfashionable in the artist's works, and so to paint a brighter, social floral scene
Philip Ball



conventional X-ray radiograph

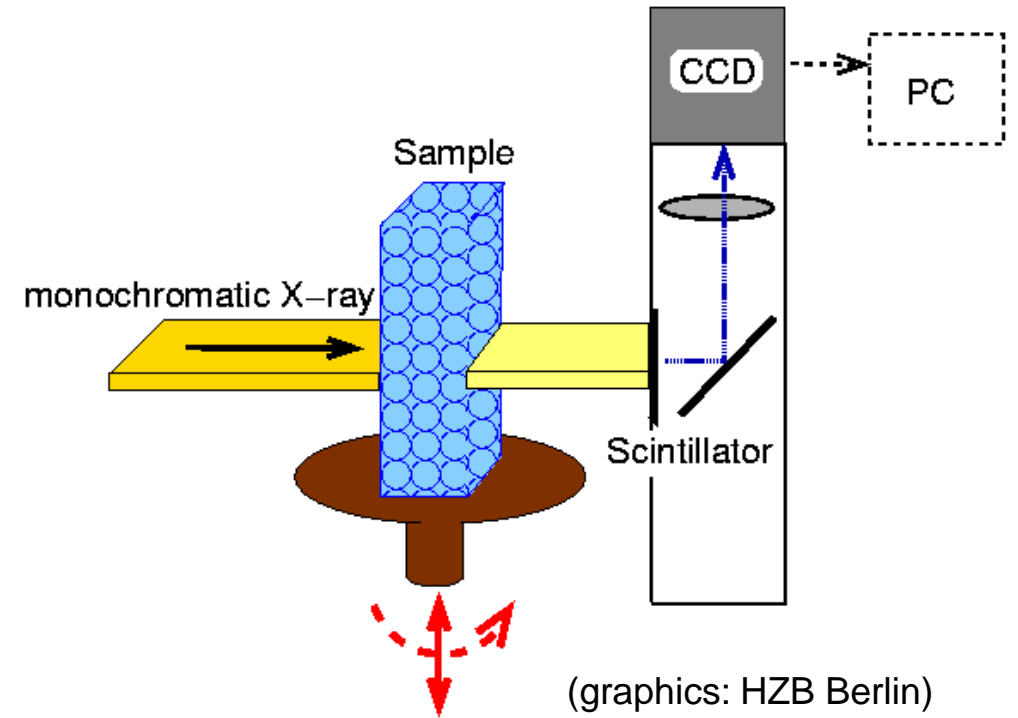


colour reconstruction based on XRF elemental mapping



other, existing painting by Van Gogh

Computed tomography (CT)



micro-tomography (μ CT)

with highly collimated synchrotron radiation
non-destructive!

resolution from μm down to **10 nm**
(with coherent imaging techniques)

Fossil insects preserved in amber (micro-CT)

Pheromones:

trigger certain social responses in members of the same species

They serve different purposes

- alarming
- aggregation
- territorial
- trail
- sex (mating)



Ulomyia fuliginosa (recent)

pheromone glands
(pocket-like pouch)

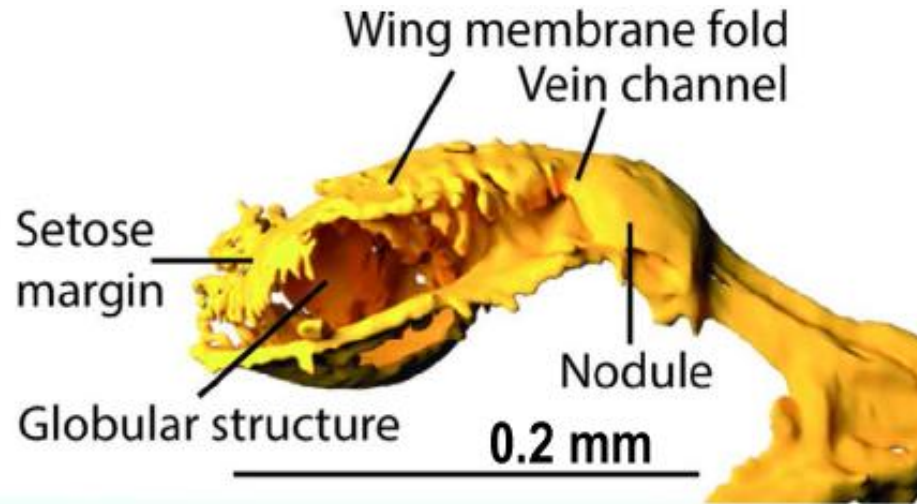
Challenge:

can we get any information relating to this from fossils?



Biting midge (Ceratopogonidae)
in 54 million-year-old Indian amber

Fossil insects preserved in amber (micro-CT)



- Pheromone releasing structures on the wings have evolved independently in biting midges
- might be much more widespread in fossil as well as modern insects than known so far
- existed already > 50 Million years ago

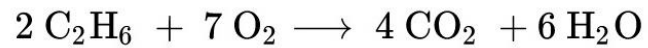
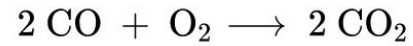
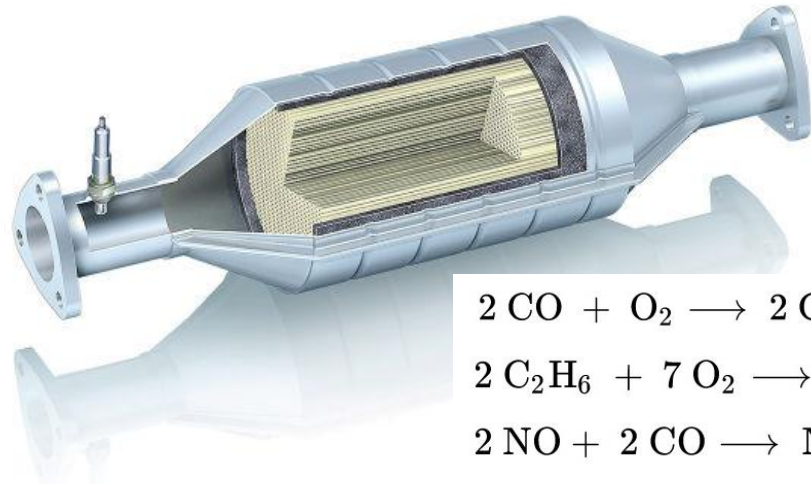


Similar to recent *Ulomyia fuliginosa* pheromones may be created by wing veins

**SR- μ CT pixel size
2.4 x 2.4 μm^2**



Aging of an exhaust gas catalyst (Pt/Al₂O₃)



Typically, the active parts of a catalyst are noble metal particles, e.g. on alumina, deposited on structured supports.

Aging of exhaust catalyst in air at 950 C:
μCT (1.27 μm voxel size) to study deactivation mechanisms (quasi “in-situ”)

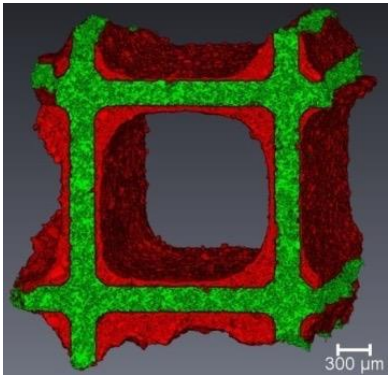
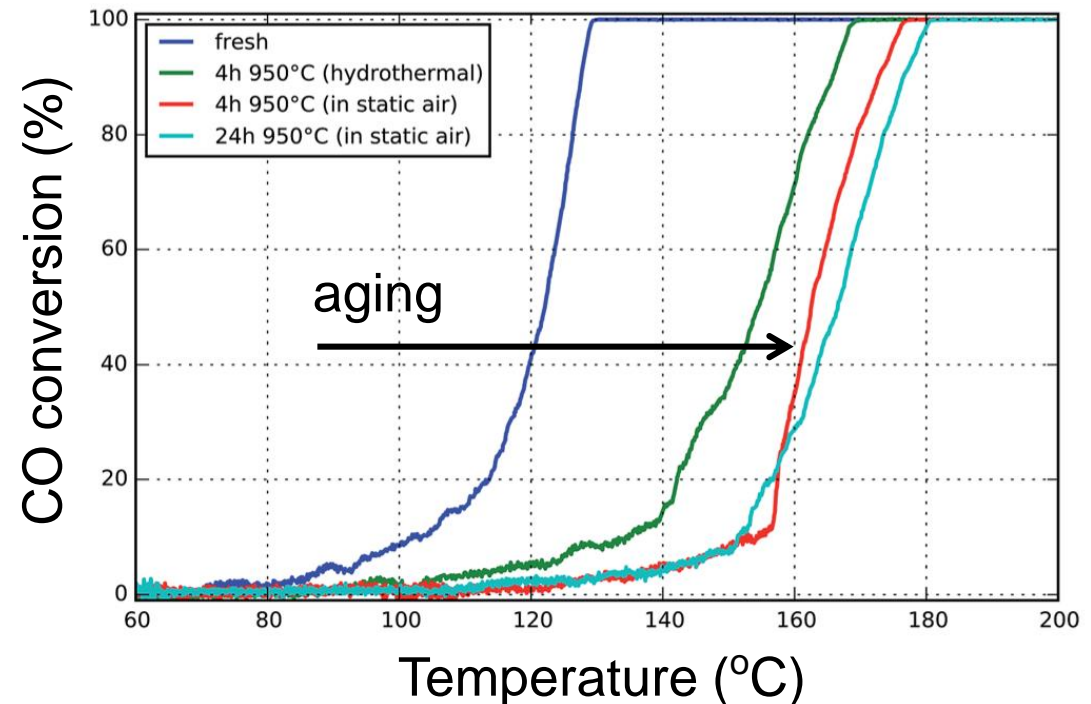
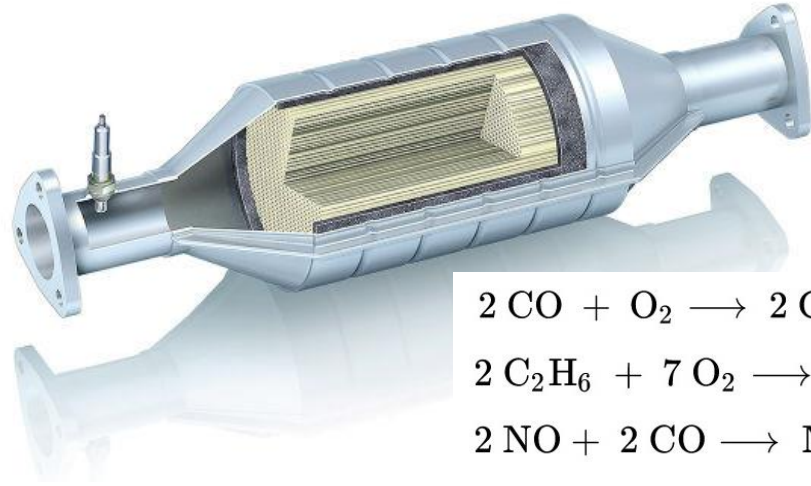


image by electron probe micro analyzer

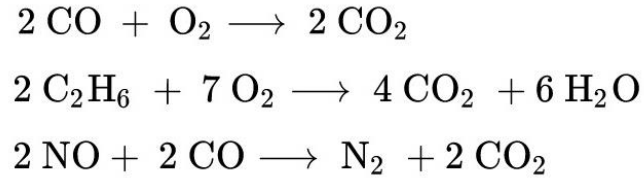
G. Hofmann et al, *RSC Adv.* 2015



Aging of an exhaust gas catalyst (Pt/Al₂O₃)



Typically, the active parts of a catalyst are noble metal particles, e.g. on alumina, deposited on structured supports.



Aging of exhaust catalyst in air at 950 C:
μCT (1.27 μm voxel size) to study deactivation mechanisms (quasi “in-situ”)

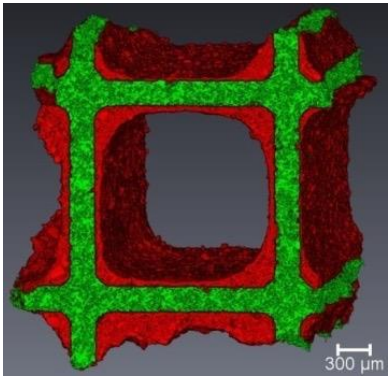
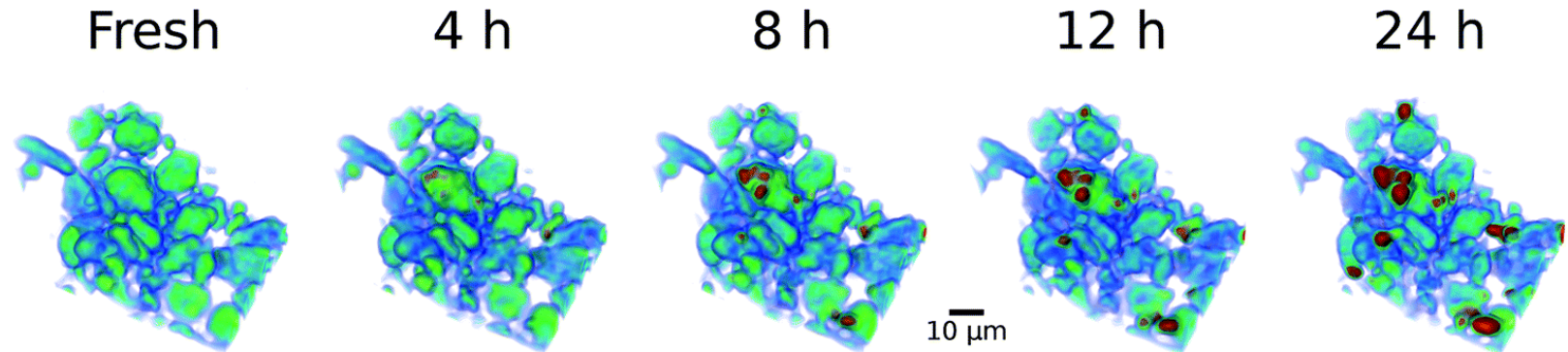


image by electron probe micro analyzer

Initially nm-sized Pt particles grow into larger crystals and agglomerate preferentially in voids between support grains



G. Hofmann et al, *RSC Adv.* 2015

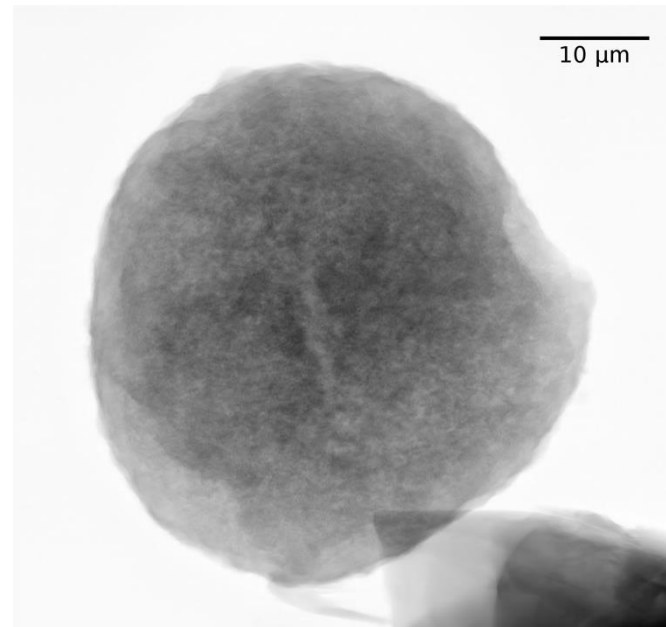
Again: catalyst aging

Fluid catalytic 'cracking'



- Conversion of the high-boiling parts of crude oil into more valuable low-boiling parts such as petrol
- Catalysts lose their effectiveness over time

Catalyst particle

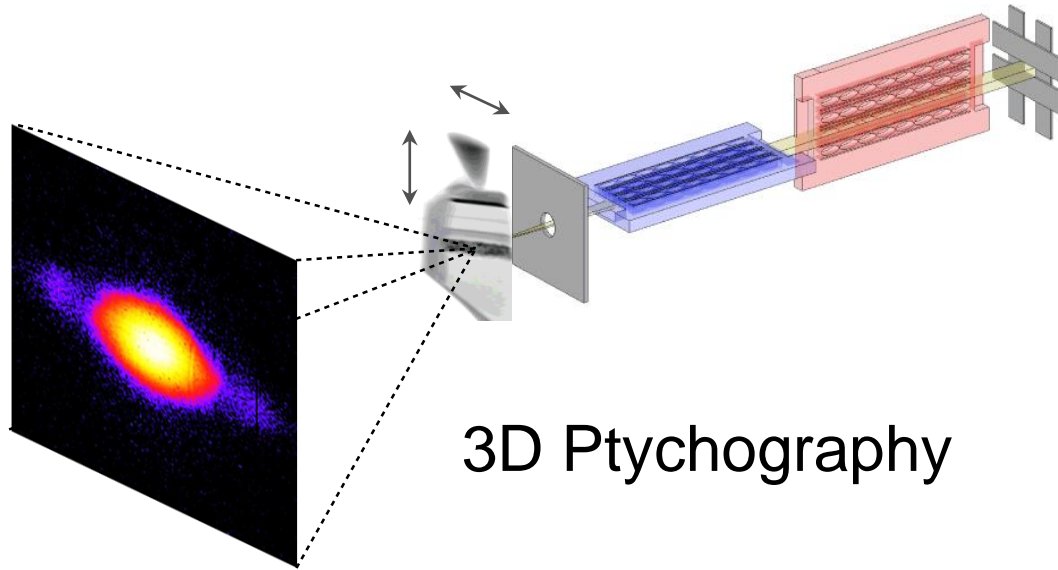


Zeolit

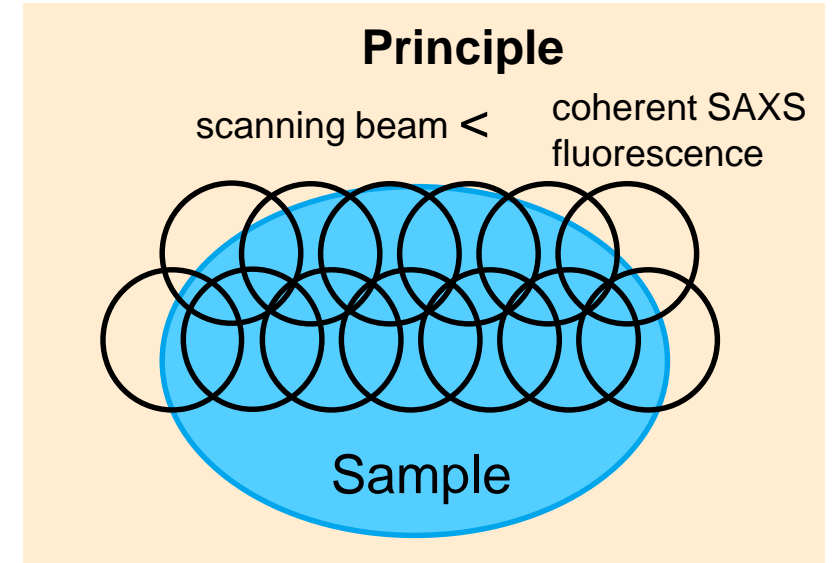
J. Garrevoet, S. Kalirai,
et al., unpublished

3D X-ray fluorescence tomography of (aged) catalytical particles

Combined X-ray ptychography and XRF imaging:
simultaneously structural and element specific data with **< 1 μm resolution**



computational imaging from
set of full-field images
with coherent illumination

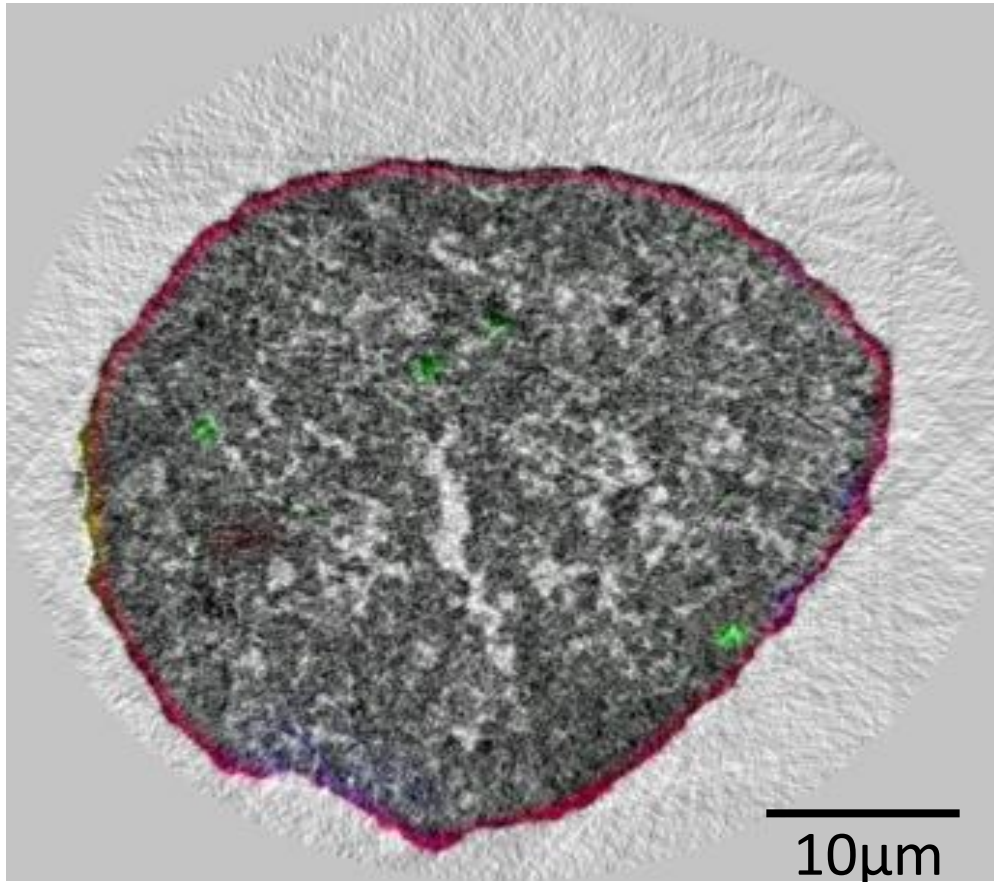


Data challenge: tomography dataset

Field of view 100 x 100 μm , beam size 300 x 300 nm
130,000 spectra/diffraction patterns per projection, 12 min/projection
178 projections \rightarrow **3 TB/tomogram** (compress. factor >40)

3D X-ray fluorescence tomography of (aged) catalytical particles

Tomographic reconstruction



Finding:
metal residuals poison the catalyst:
transport into the particle is
clogged by built up of Fe/Ni layer

Simultaneous reconstruction of
element distribution:

- Fe
- Ni
- Ti
- Ga (marker)

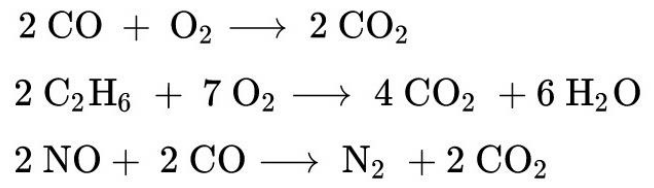
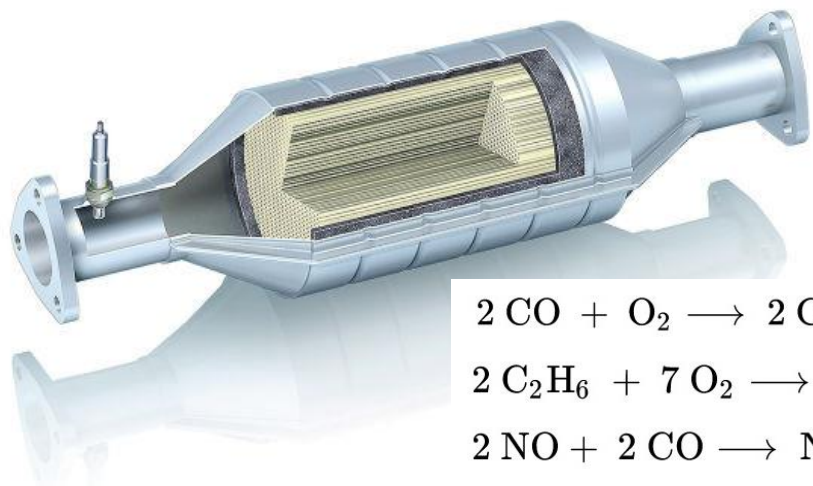
resolution (by beam size): **300 nm**

structural data (electron density):
resolution (by ptychography): **<100nm**

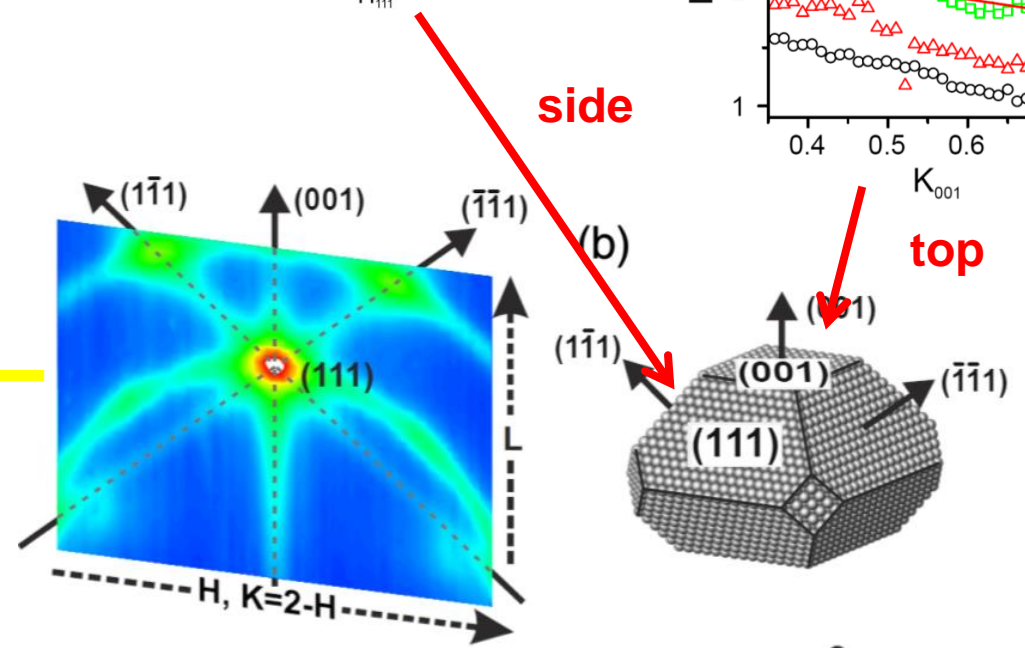
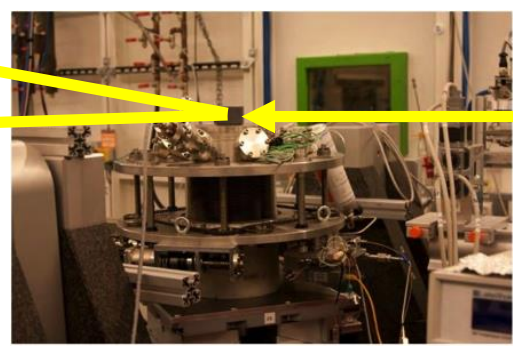
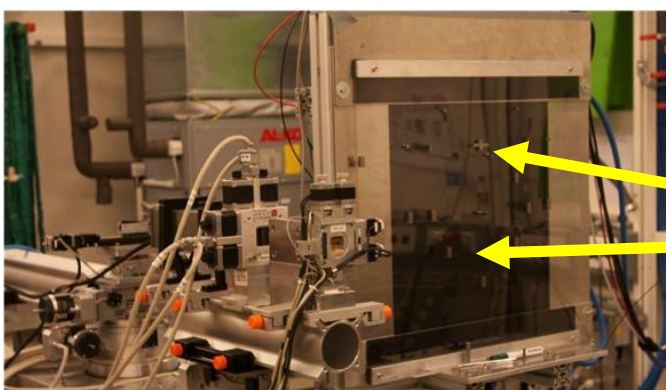
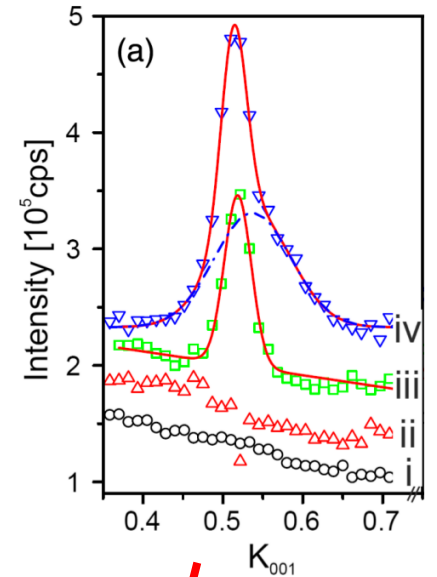
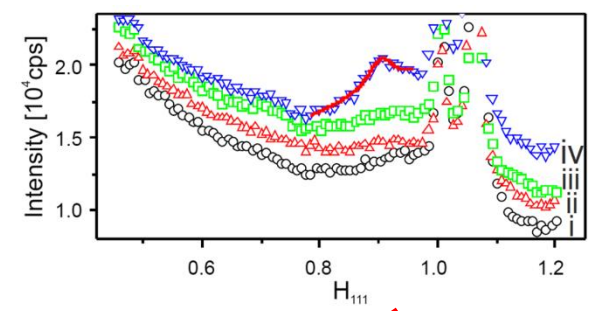
J. Garrevoet, S. Kalirai et al. (2017)

Catalyst at work on the atomic scale

study of catalytic under realistic conditions
with structural information on the atomic scale



CO oxidation over PtRh nano particles
in-situ X-ray diffraction during the
catalytic process



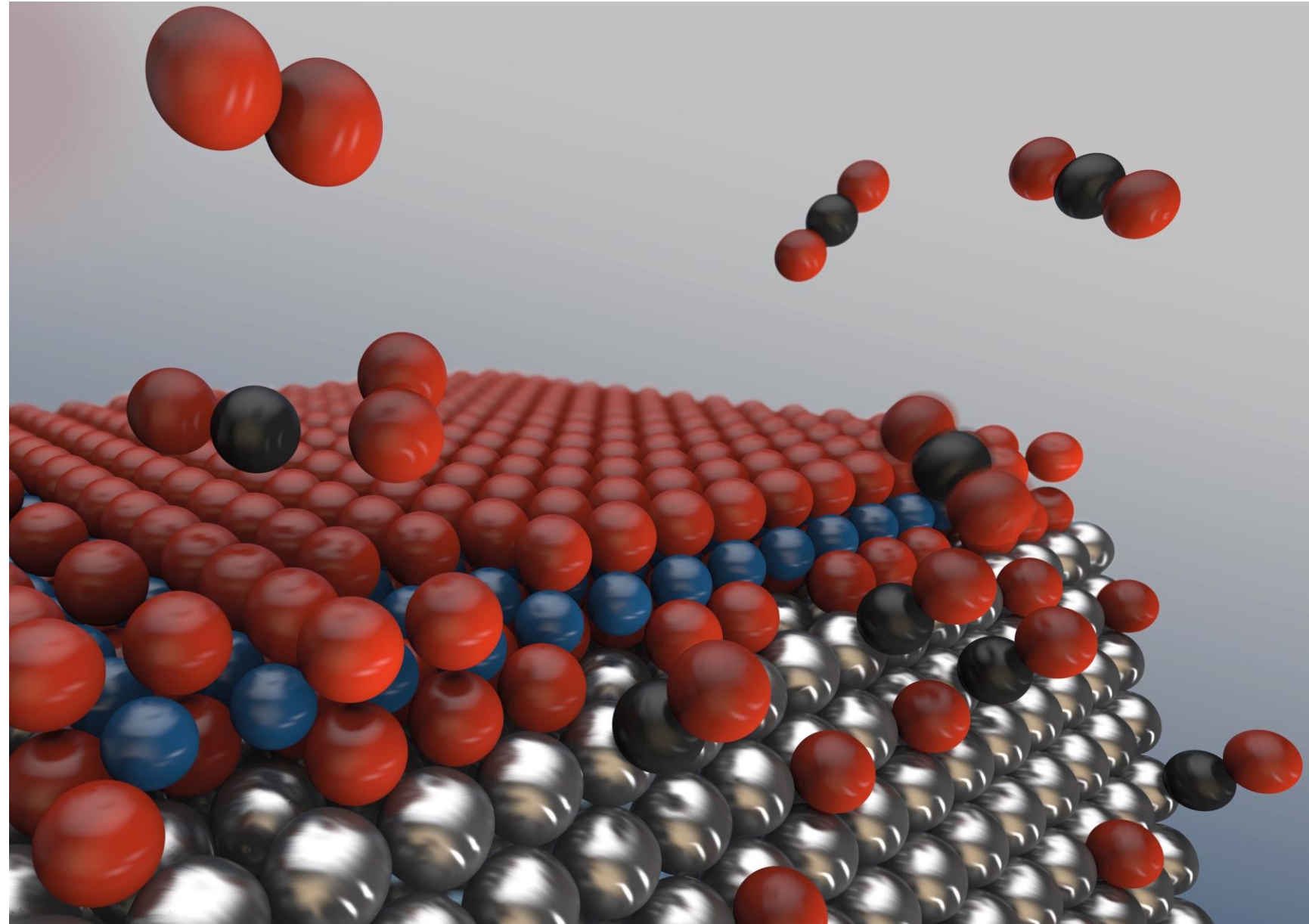
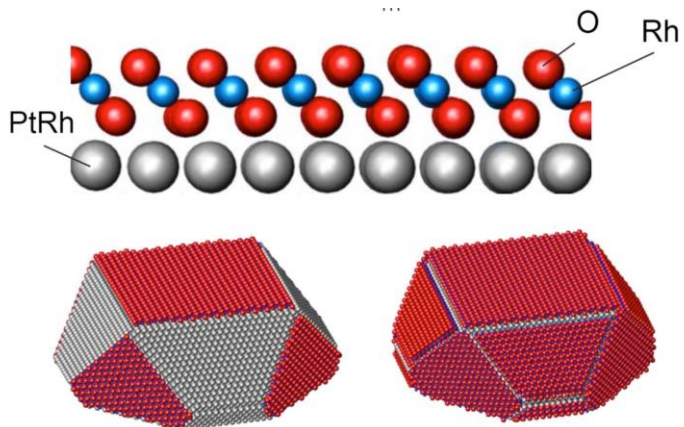
Hejral et al., PRL (2018)

Catalyst at work on the atomic scale

Increasing O₂ (red) concentration:
→ O-Rh-O sandwiches form
→ CO → CO₂ reaction inhibited

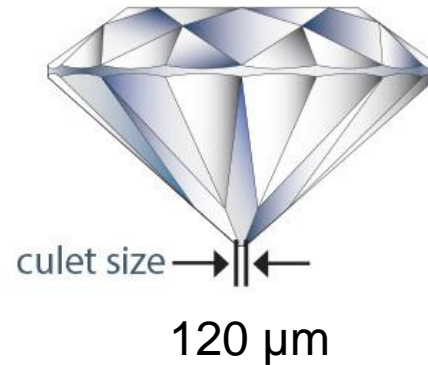
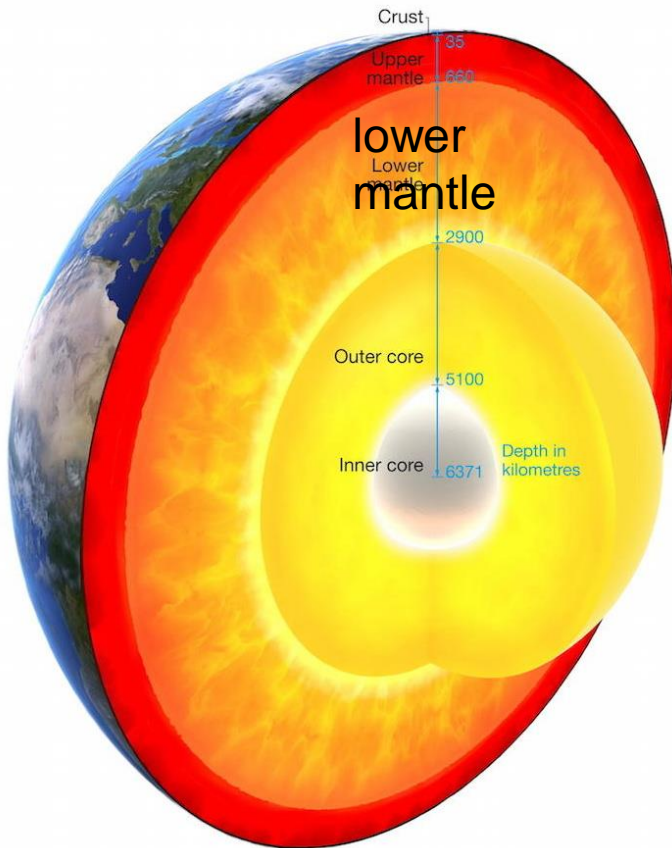
At the edges:
sandwiches brake up
→ free active sites for catalysis

Conclusion:
more edges
→ more catalytic efficiency



Materials under extreme conditions

- structure and dynamics of our planet ?
physical and chemical properties of lower mantle
- try to generate similar conditions in the lab
- lower mantle: about $\frac{1}{2}$ the Earth volume
~80% is bridgmanite $[(Mg,Fe)(Si,Al)O_3]$

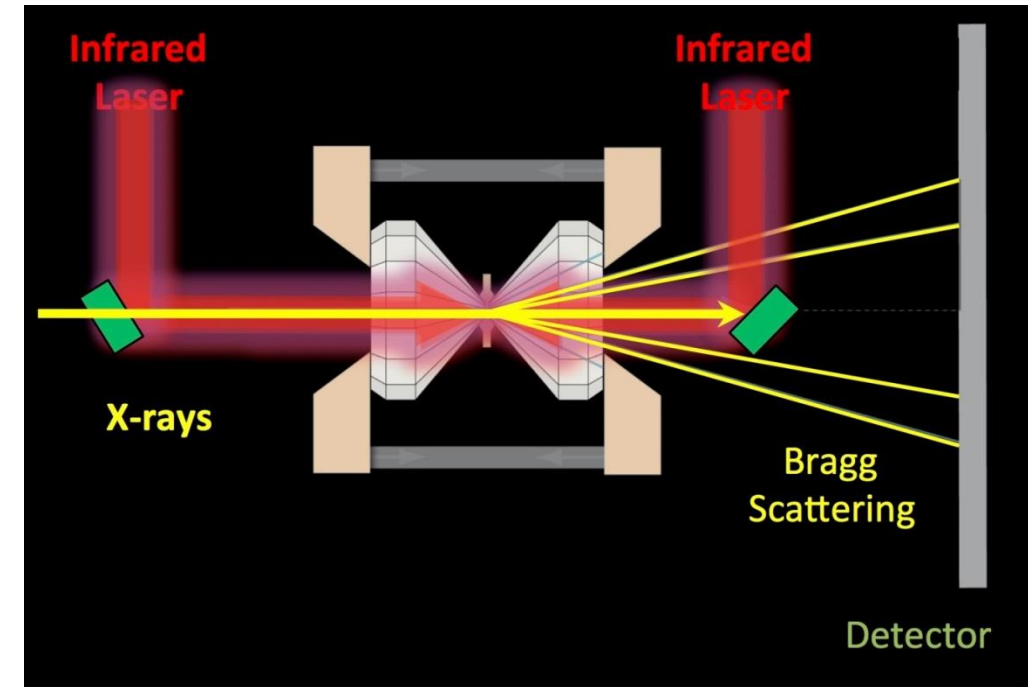


bottom of the lower mantle
(~2900km):

pressure ~136 GPa (1.4 Mbar)
temperature ~ 3000 K

Experiment:

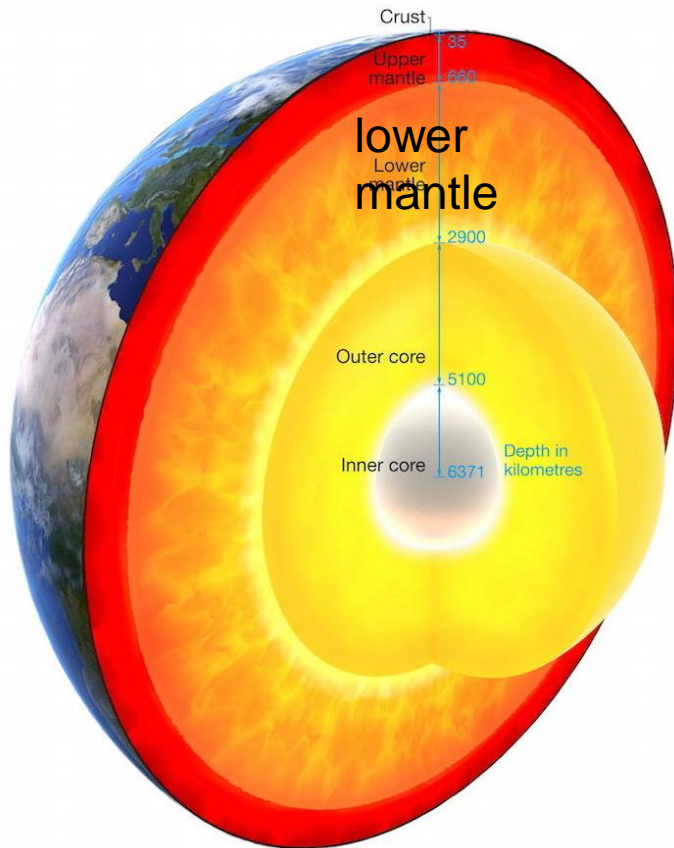
- **laser-heated diamond anvil cell**
- brilliant synchrotron X-rays for diffraction
- crystal size $\sim 10 \times 10 \times 5 \mu\text{m}^3$
- **X-ray beam size $\sim 3 \times 5 \mu\text{m}^3$**



range: 32 to 130 GPa
2200 to 3100 K

Materials under extreme conditions

- structure and dynamics of our planet ?
physical and chemical properties of lower mantle
- try to generate similar conditions in the lab
- lower mantle: about $\frac{1}{2}$ the Earth volume
~80% is bridgmanite $[(\text{Mg,Fe})(\text{Si,Al})\text{O}_3]$



bottom of the lower mantle
(~2900km):

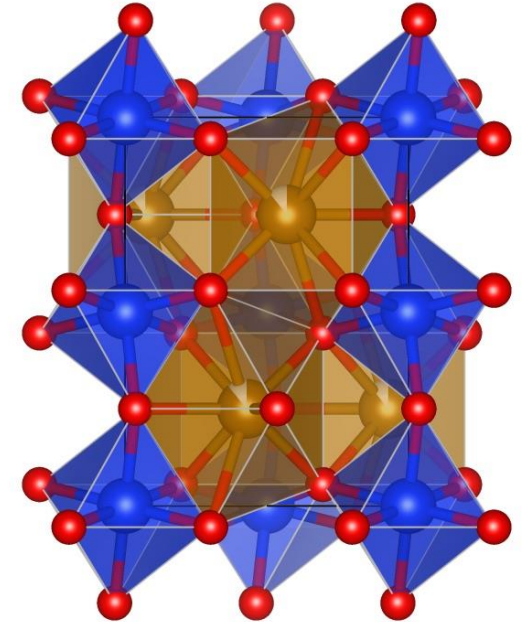
pressure ~136 GPa (1.4 Mbar)
temperature ~ 3000 K

very few data on bridgmanite structure under these conditions & inconclusive results

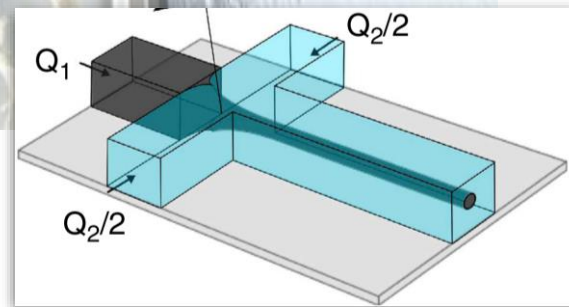
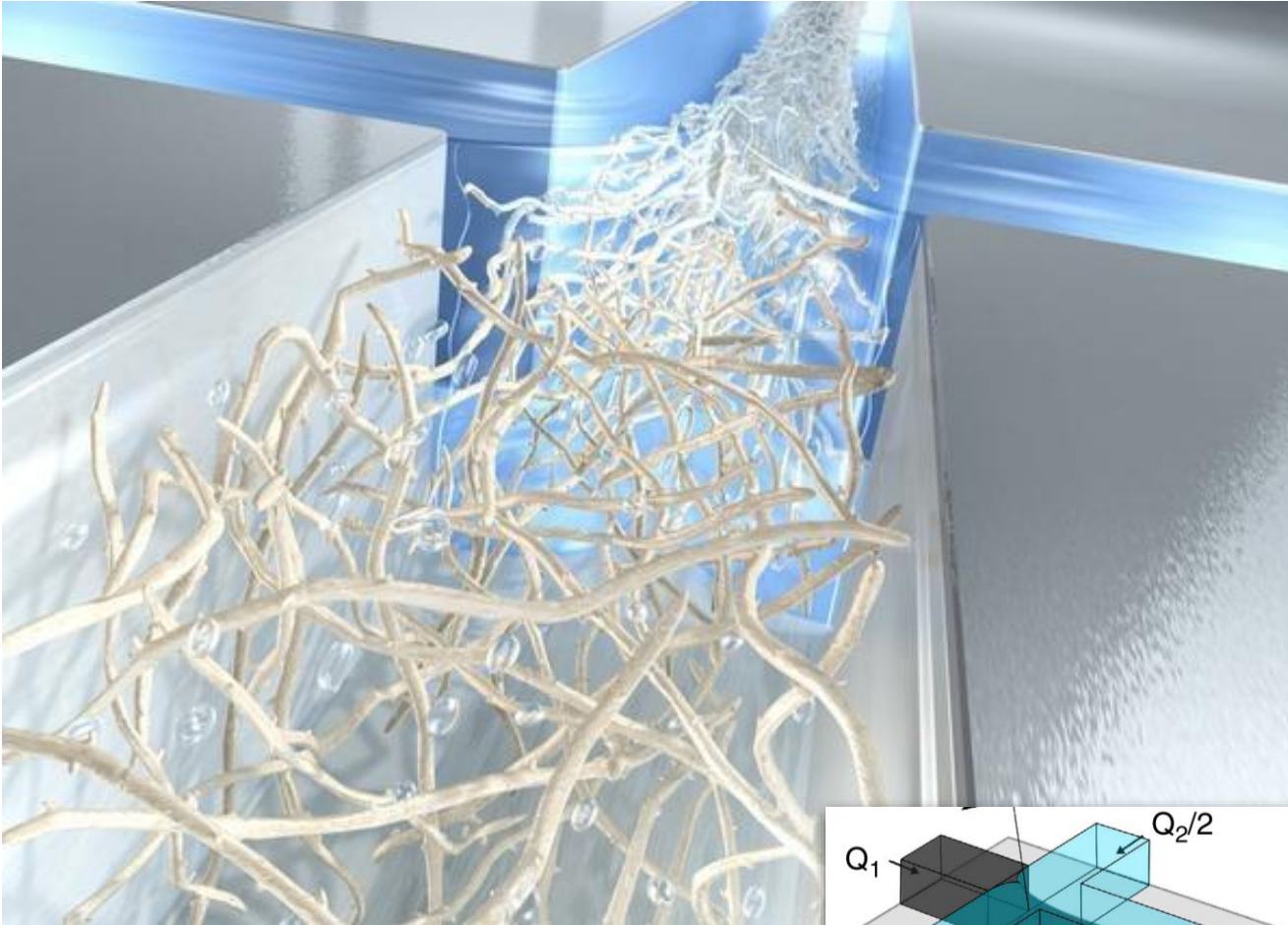
Result here:

- bridgmanite forms Fe-bearing varieties (not synthesized before)
- stable up to 120 GPa and 3000 K
- compressibility is different from any known bridgmanite

→ **direct implications for interpretation of seismic data**



Learning from nature: biomimetic materials from cellulose



Cellulose nano fibrils:

- > Building blocks for bio-based materials
- > Nanostructure determines material properties (controlled fabrication needed)

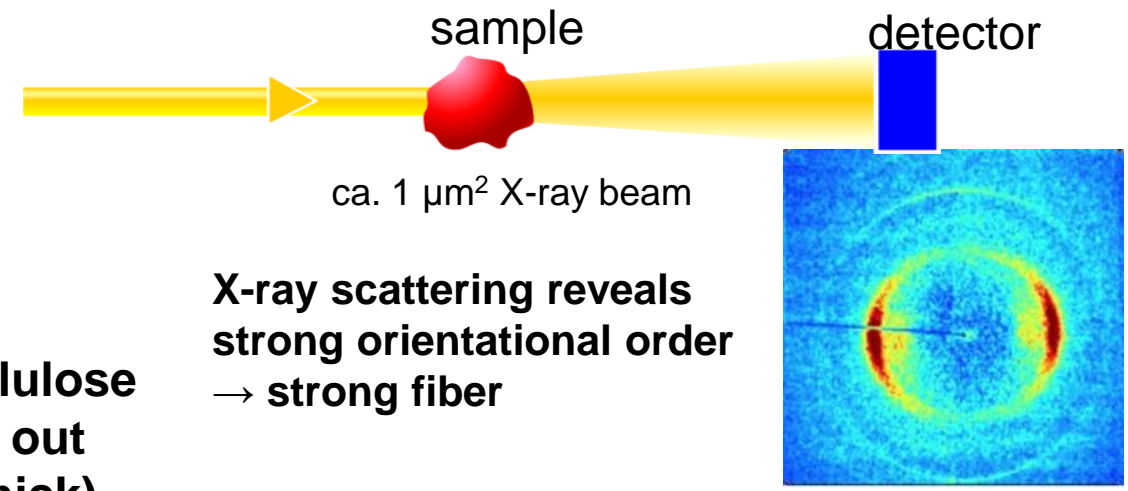
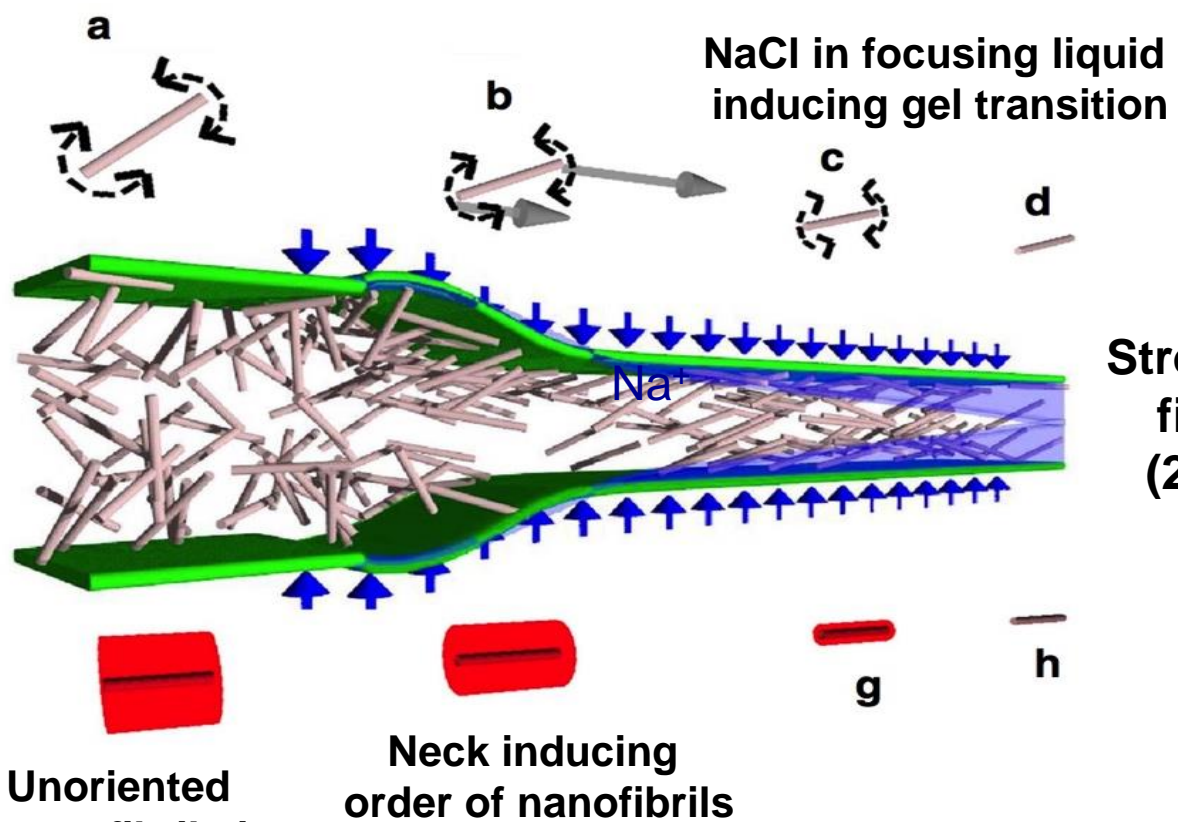
Here:

- > Use hydrodynamic alignment with dispersion-gel transition
- > fibril orientation controlled by process parameters

Result:

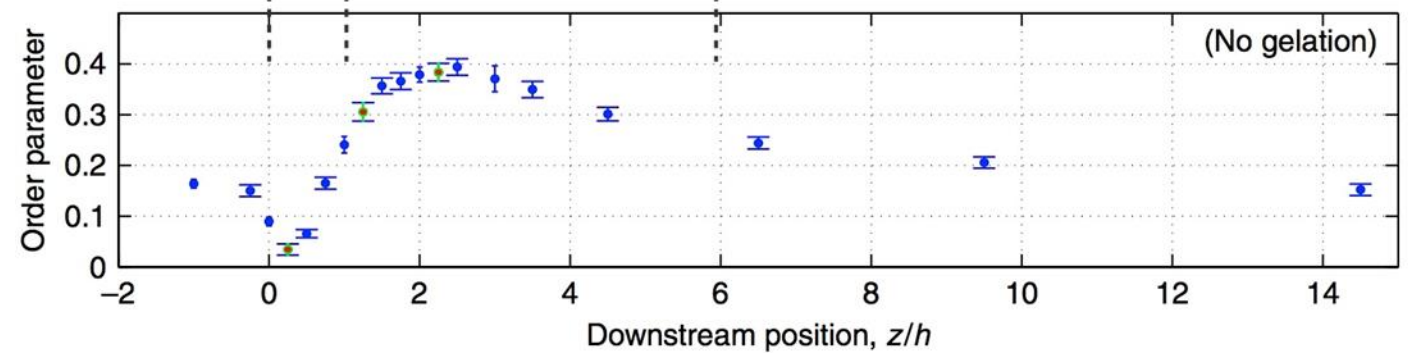
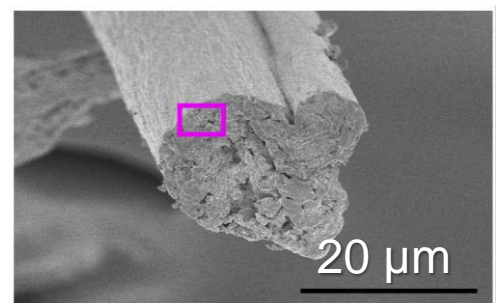
- > specific ultimate strength highest among filaments made of nanofibrils (comparable to wood)

Microfluidic alignment of nano fibrils



X-ray scattering reveals strong orientational order \rightarrow strong fiber

Strong cellulose filament out (20 μm thick)

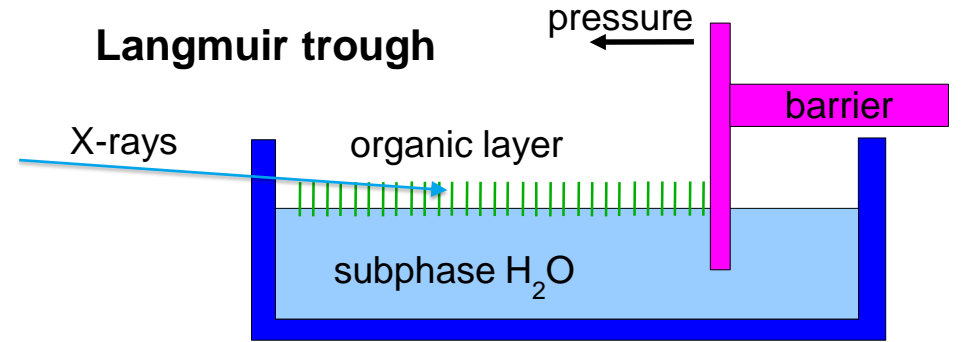
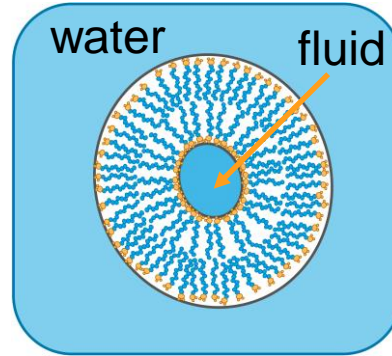
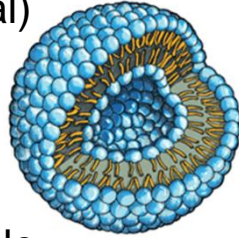


K. M. O. Håkansson, et al., Nature Commun. 5, 4018 (2014).

Towards controlled drug delivery inside the body

Tailored vesicles from lipid membranes

- > Vesicles are natural containers (surface tension: typically spherical)
- > Potential medical application in drug delivery
- > Difficulty:
 - spherical vesicles are very stable
 - no “break on demand” for medical applications

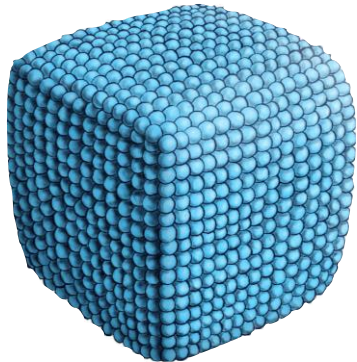


Grazing Incidence X-ray diffraction

- > reveals the in-plane structure
- > depending on pressure

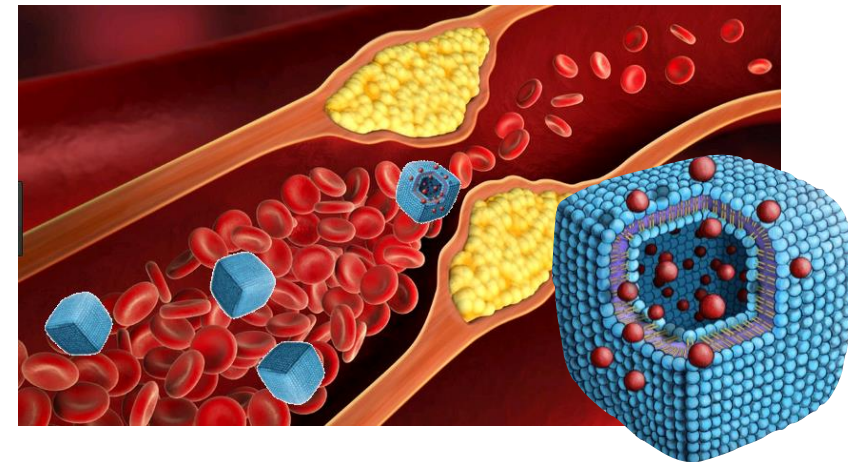
Here: **very stiff lipid** (1,2-diamidophospholipid)

- opposes bending
- **cubic vesicles**



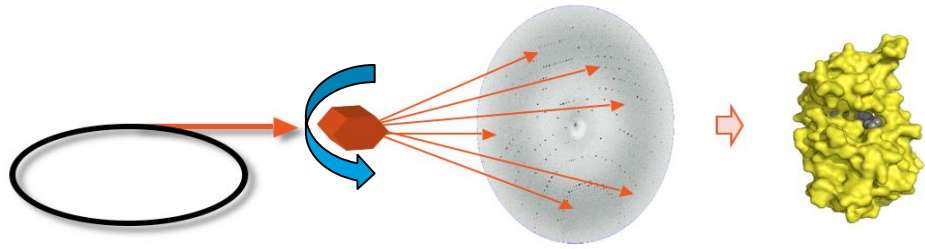
What molecular structure creates this effect?

- > Already crystalline at very small pressures
- > vesicle can be designed to break easily at edges
- > good for drug delivery

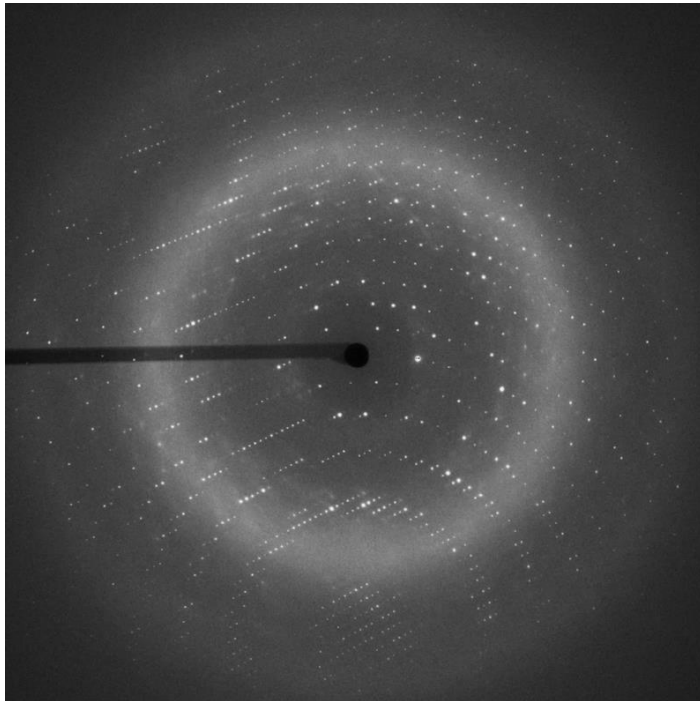
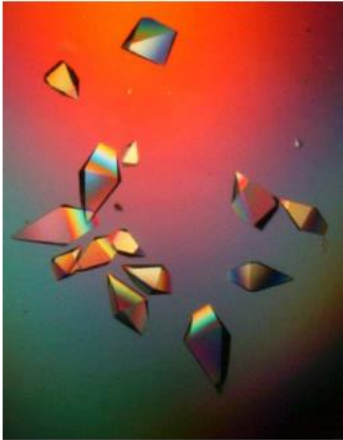


F. Neuhaus, et al. Angew. Chemie Int. Ed. **56**, 6515 (2017)

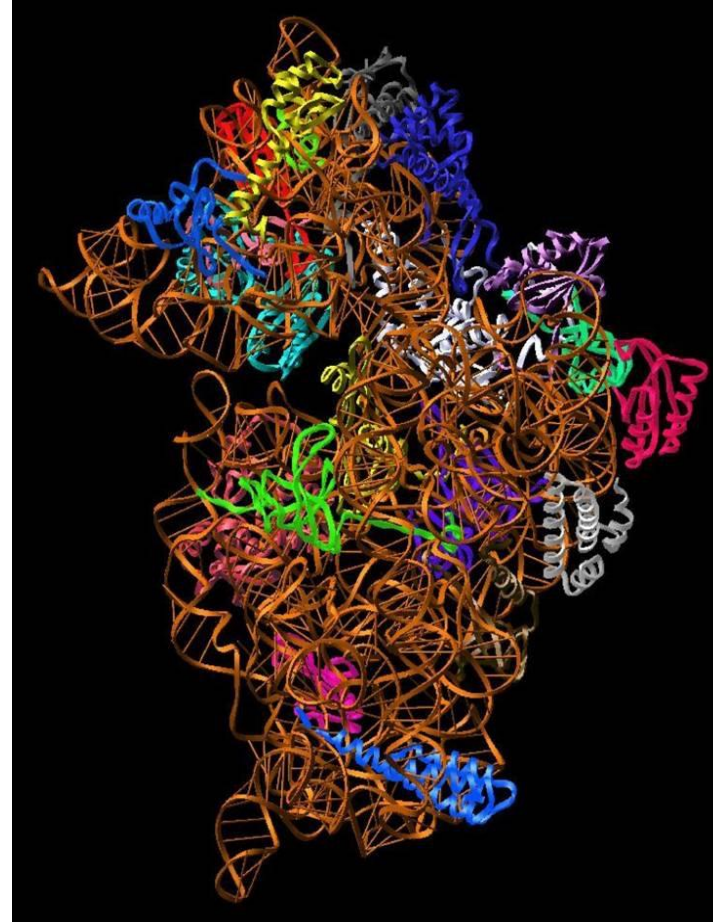
Life sciences: detailed structure of macro molecules



Diffraction of bright, well collimated X-rays
ideal for structure determination of
(μm -sized) crystals of bio material



Structure of the Ribosome molecule



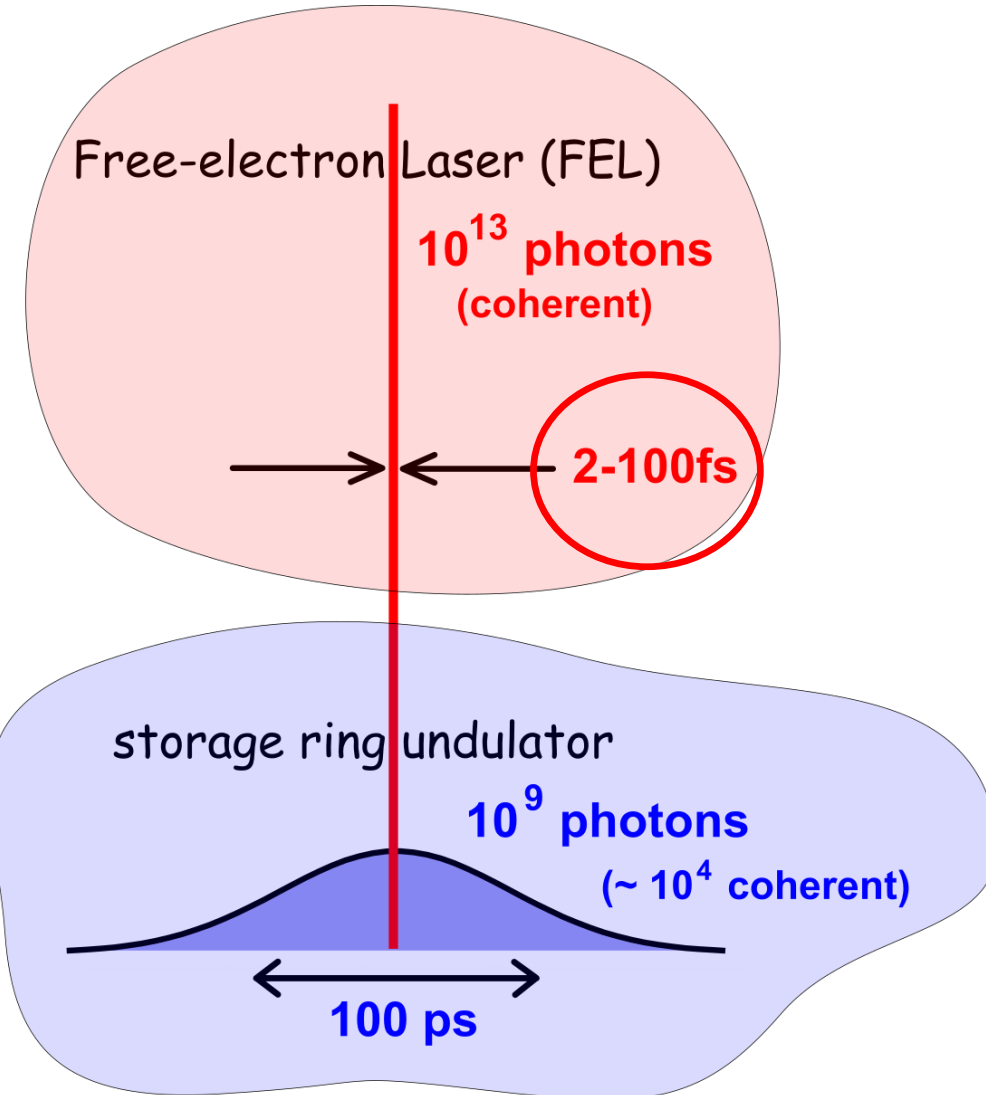
Ada Yonath
Nobel prize in
chemistry (2009)

Detour: new X-ray sources: Free-Electron Lasers

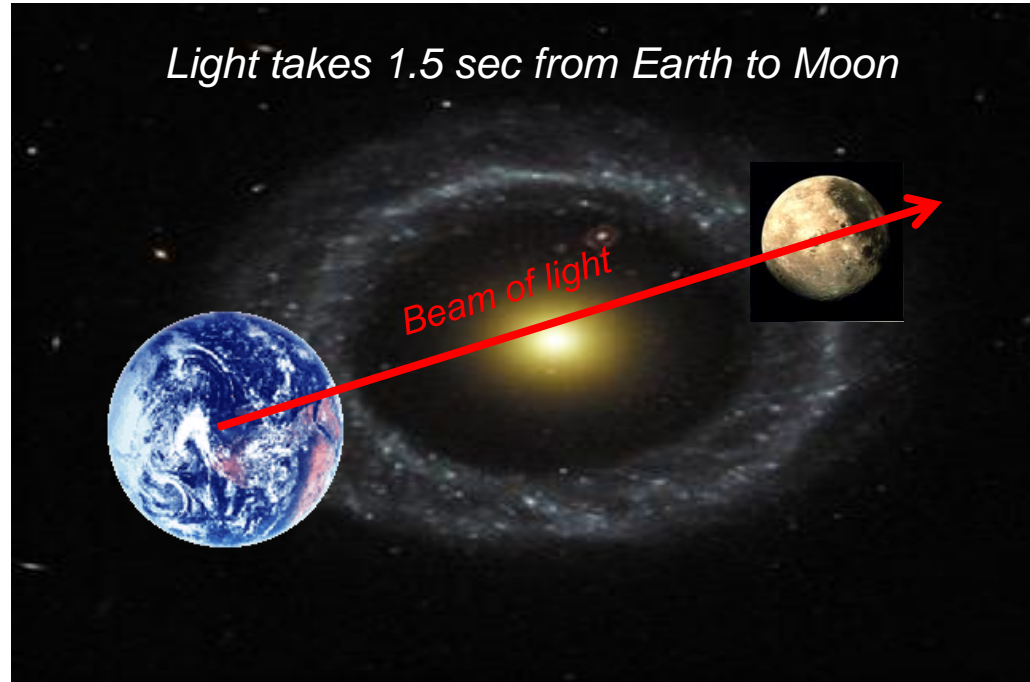
Linear electron accelerators with undulators producing **ultra-short and intense** X-ray pulses



e.g. the new European XFEL (Hamburg)

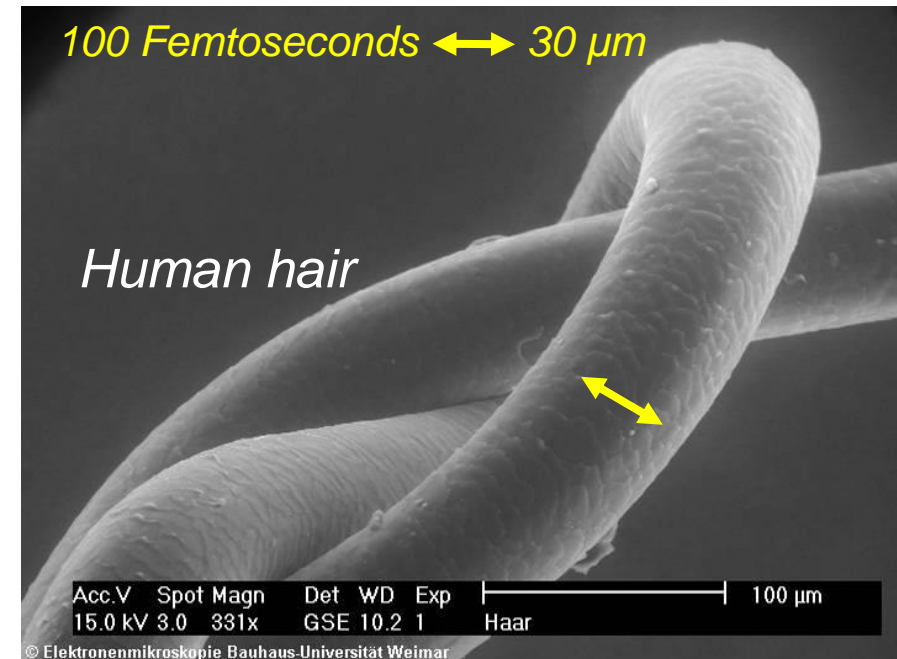


How short is short?

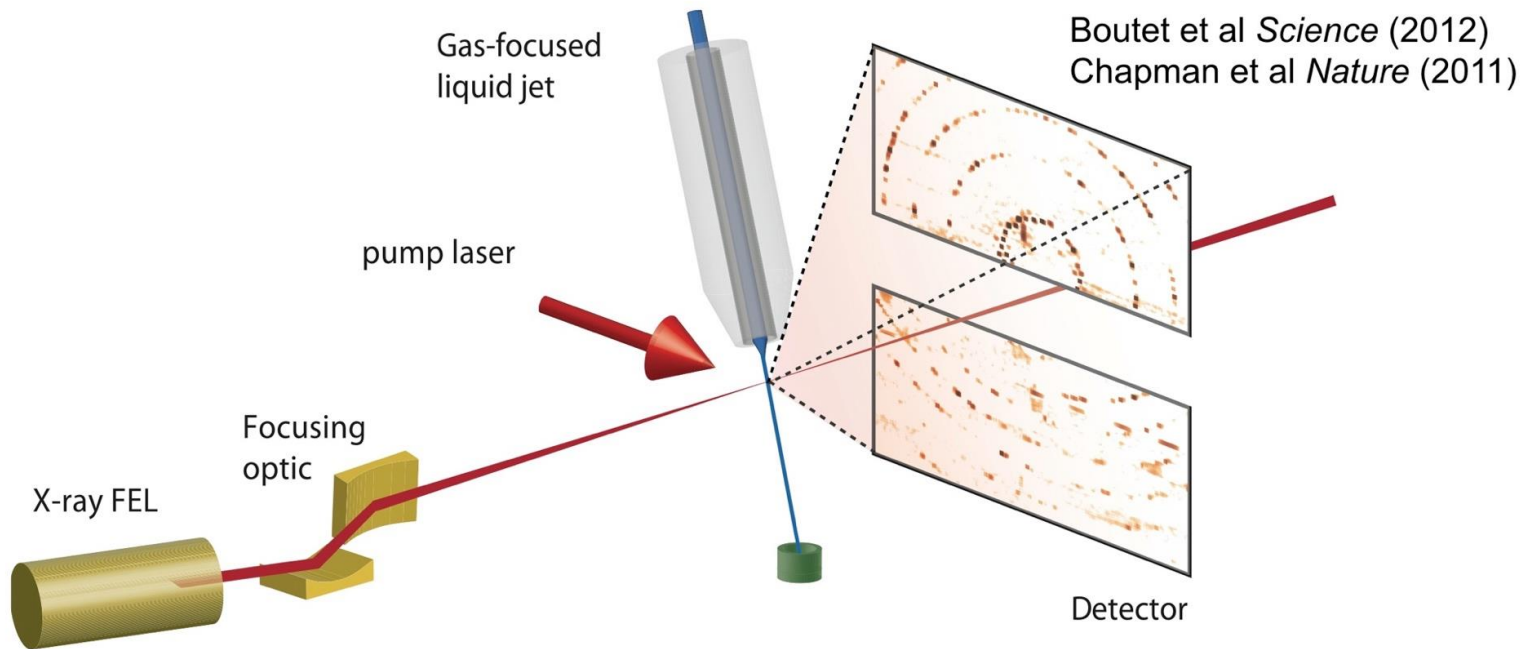


100 fs

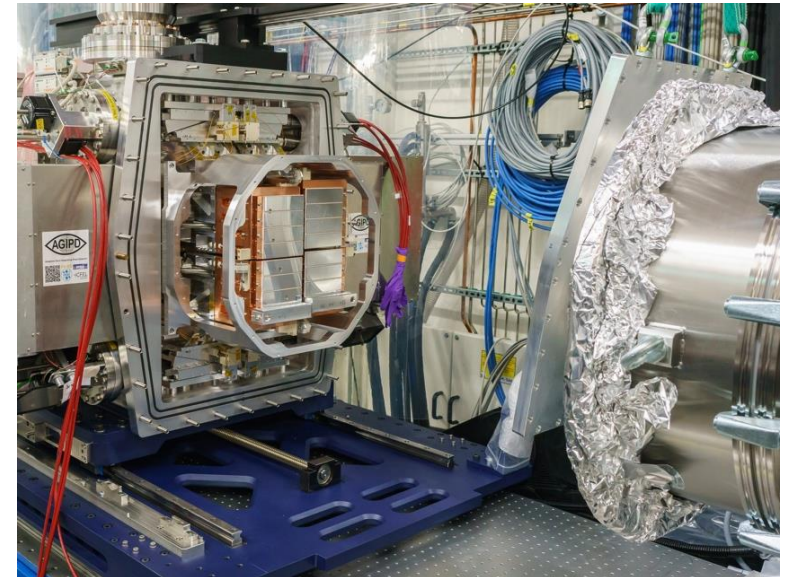
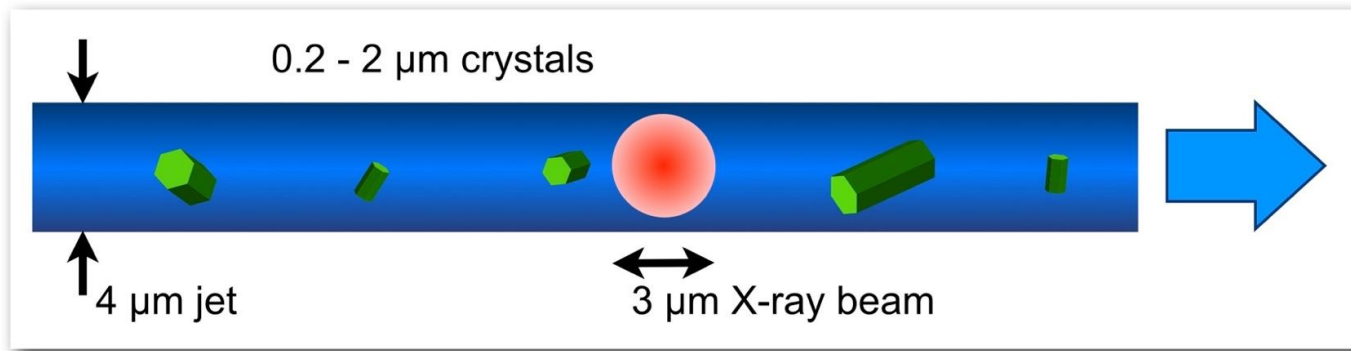
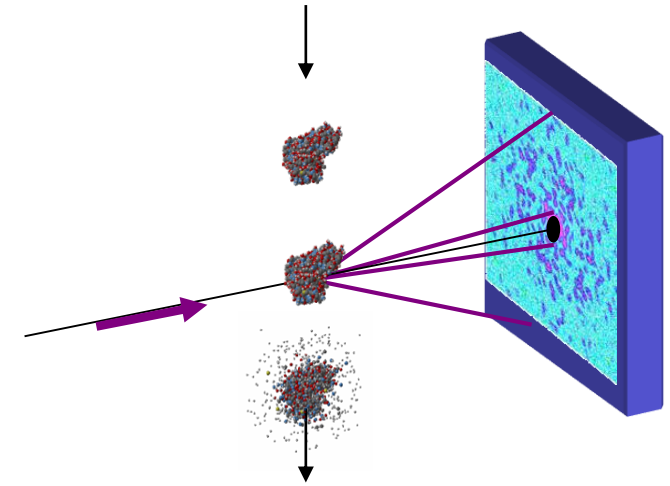
Speed of light: ~300000 km/s



Serial femto-second crystallography

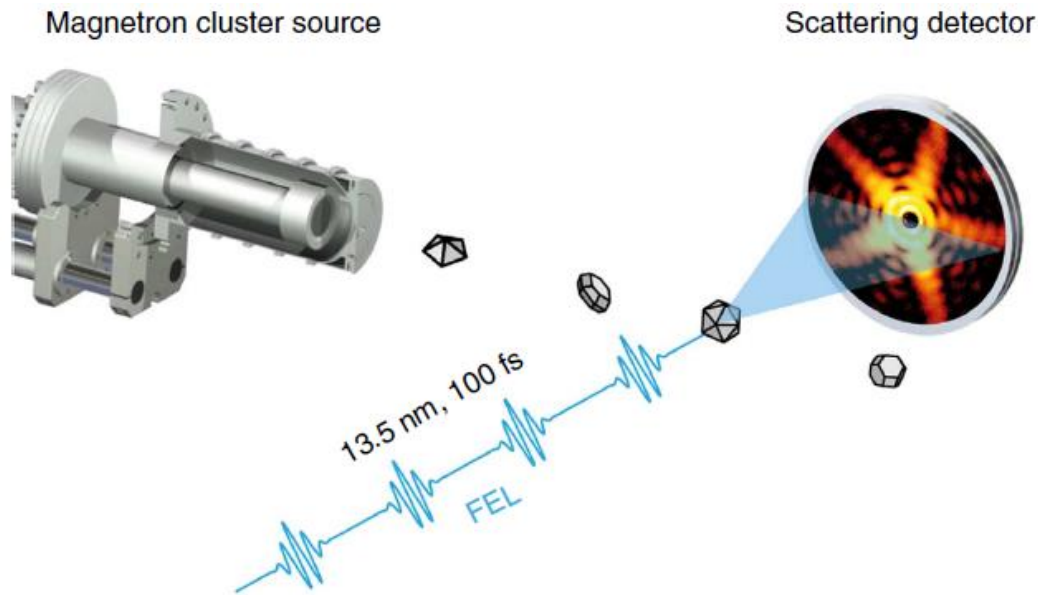


particle is destroyed by the X-ray pulse
BUT: the structural information is obtained,
before it „falls apart“

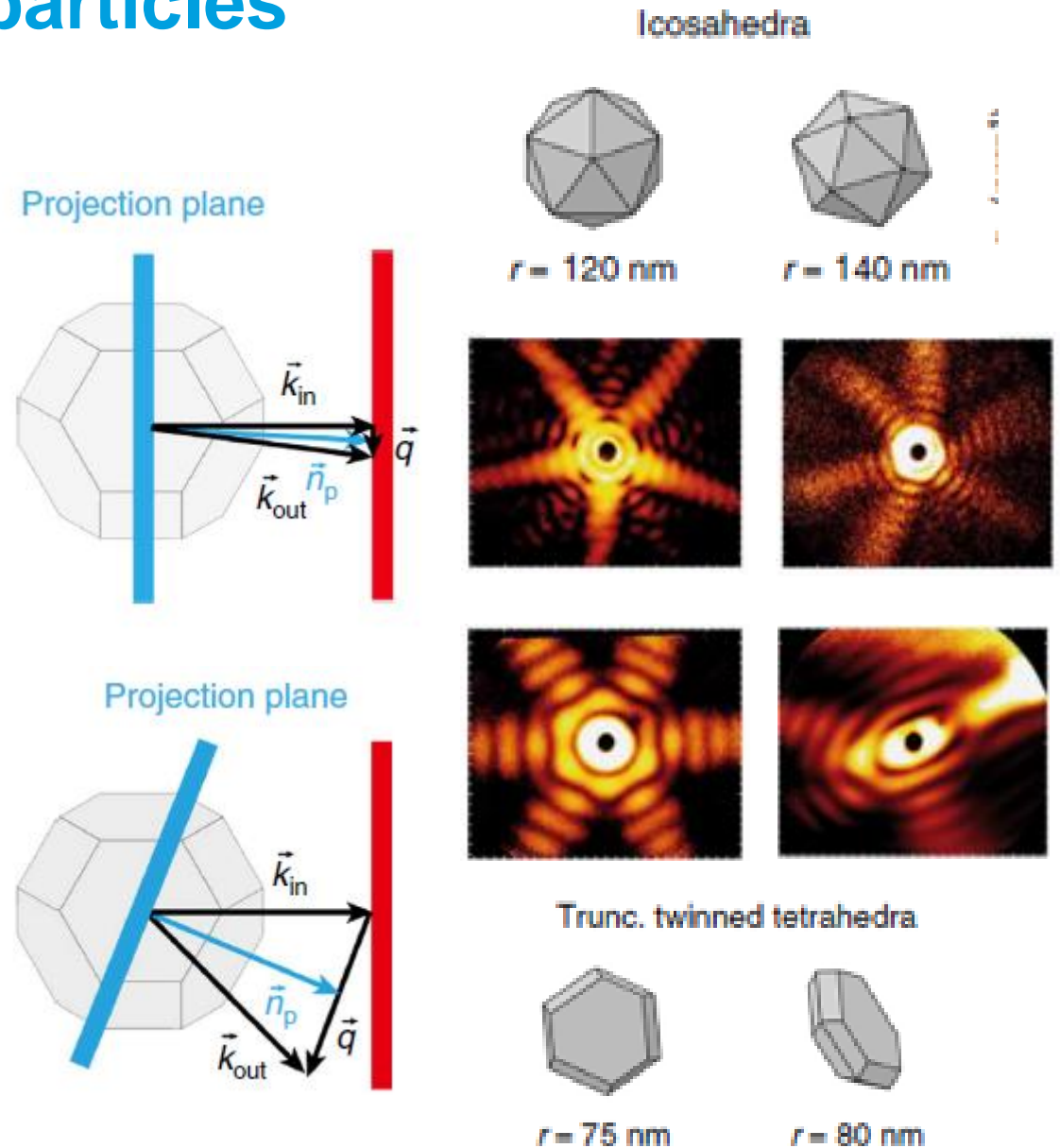


3D Imaging of Individual Ag Nanoparticles

Single „shot“ imaging of metastable states with specialized 2D detectors



Numerous highly symmetrical three dimensional shapes revealed, including several types known as Platonic and Archimedean bodies



**At the end:
Summary of what has
not been talked about**

Applications of SR X-ray techniques in materials' science



Energy & Climate

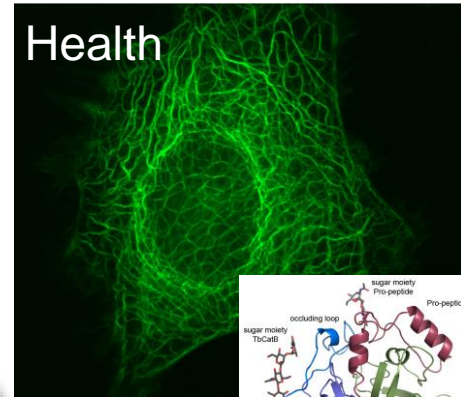
- > generation (sun, wind, water, gas, ...)
- > storage (batteries, hydrogen, ...)
- > transport (super-conducting power lines)

electronic, magnetic, optical properties of nanostructured functional materials

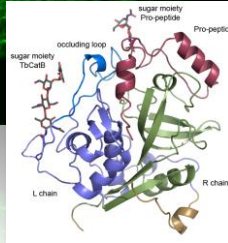
chemistry, catalysis (from macroscopic to atomic length scales)

structure-based rational drug design (atomic scale structure & dynamics)

Building blocks of life
> structure
> function



Health



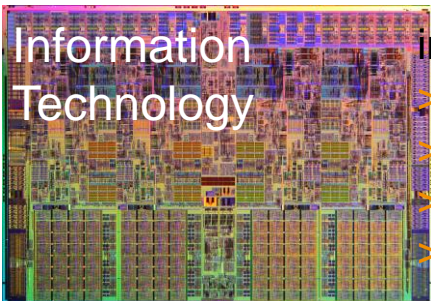
Understanding the Complexity of Matter

extreme states of matter (extremely small volumes)

tailored mechanical properties, engineering (down to nanoscale)

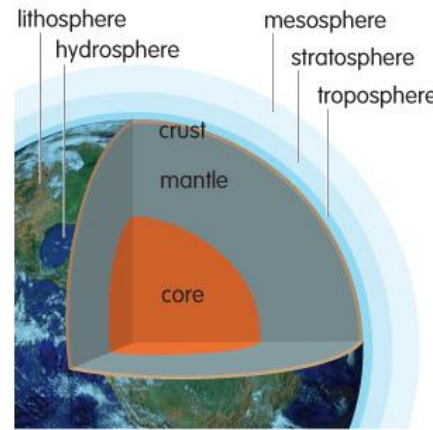
tribology

materials design



Information Technology

- information:
- > processing
 - > sensors
 - > exchange
 - > storage



earth & environment:

- > natural resources
- > volcanos and earthquakes
- > pollution
- > ...



Transport

- > efficiency (light-weight structures, propulsion, ...)
- > safety

Thank you for
your attention

